



Predicting Resilient Modulus of Unsaturated Subgrade Soils Considering Effects of Water Content, Temperature, and Hydraulic Hysteresis

Masood Abdollahi, S.M.ASCE¹; and Farshid Vahedifard, F.ASCE²

Abstract: The resilient modulus, M_R , of subgrade soils is an important parameter in design and analysis of pavements. Subgrade soils are often unsaturated and can experience a wide range of suctions due to changes in water content and temperature induced by seasonal variation and climatic events. Laboratory- and field-measured data show that M_R is affected by stress level, water content, temperature, and hydraulic hysteresis. However, none of the existing models explicitly accounts for the effect of temperature nor can they accurately predict M_R in high suctions. In this study, a generalized model is developed that can predict M_R while incorporating water content, temperature, changes in deviatoric stress, and hydraulic hysteresis. A base model is first presented to predict the variation of M_R in regard to water content and is dictated by two distinct water retention mechanisms—capillarity and adsorption. Accordingly, a two-part model is employed to separately account for changes in M_R with water content under capillary and adsorption mechanisms. This feature allows the proposed model to accurately capture the characteristics of M_R over the entire range of suction. The base model is then extended to incorporate the effects of temperature, changes in deviatoric stress, and hydraulic hysteresis. The proposed model exhibited an excellent performance upon validation against a total of 218 experimentally measured M_R values reported in the literature spanning 14 different test sets on nine different soils tested under different conditions. The predictive errors are significantly lower than that from four alternative models, including the model in the *Mechanistic-Empirical Pavement Design Guide* (MEPDG). The presented model is straightforward and can be used in practice to predict the M_R of subgrade soils considering concurrent changes in water content and temperature. **DOI:** 10.1061/(ASCE)GM.1943-5622.0002244.

Author keywords: Unsaturated soil; Pavement; Resilient modulus; Subgrade soil; Suction; Temperature; Deviatoric stress; Hydraulic hysteresis; Adsorption.

Introduction

Design and analysis of pavements mainly rely on the resilient modulus, M_R , of subgrade soils (e.g., AASHTO 2003; NCHRP 2004). Seed et al. (1962) first introduced the resilient modulus as the ratio of applied deviatoric stress (σ_d) to the recoverable strain (ε_r), characterizing the stiffness and stress–strain behavior of subgrade soil under cyclic traffic loading. Several studies have shown that M_R of subgrade soil is not a constant material property but affected by different factors including the soil type, stress state, water content or suction level, temperature, number of load repetition, and wetting and drying cycles (e.g., Fredlund et al. 1977; George 2004; Puppala 2008; Liang et al. 2008; Caicedo et al. 2009; Khoury et al. 2012; McCartney and Khosravi 2013; Ng et al. 2013; Ng and Zhou 2014; Han and Vanapalli 2016; Zhang et al. 2021; Blackmore et al. 2020). For instance, it is shown that M_R increases with an

increase in confining pressure and suction and decrease in deviatoric stress and water content.

Repeated load triaxial (RLT) testing, designed to simulate traffic loading, has been extensively used in literature to investigate the effects of water content and stress level on M_R (e.g., Khoury and Zaman 2004; Yang et al. 2005; Liang et al. 2008; Sawangsuriya et al. 2009; Yao et al. 2018). In the conventional form of RLT testing, suction measurement is conducted independently and after completion of the test, an approach that ignores the effects of stress level and suction on each other. More recent efforts have conducted RLT tests under suction-controlled conditions using techniques such as the axis-translation method (e.g., Cary and Zapata 2011; Ng et al. 2013; Zhang et al. 2021). Almost all of these experiments were only able to apply suction up to 1,000 kPa. However, subgrade soils, due to the presence of fine-grained particles, can experience much higher suctions, which can considerably affect pavement performance. For example, Puppala et al. (2011) measured suctions of nearly 8 MPa in subgrade soil at a site in San Antonio, Texas, while studying the circumstances in which cracking occurs. Banerjee et al. (2020a, b) employed different suction imposition techniques to conduct RLT tests on silt and clay samples over a wide range of suctions. Test results reported by Banerjee et al. (2020a, b) showed that the suction hardening of M_R at high suction values exhibits a different trend compared with low suction values being much more pronounced in high suctions.

In addition to inducing changes in water content and suction, seasonal changes impose subgrade soils to a wide range of temperatures in different climates. Further, extreme climatic events such as prolonged droughts, heatwaves, ice jams, snowstorms, and

¹Ph.D. Student, Richard A. Rula School of Civil and Environmental Engineering, Mississippi State Univ., Mississippi State, MS 39762. ORCID: https://orcid.org/0000-0002-5273-2073. Email: ma1882@msstate.edu

²CEE Advisory Board Endowed Professor and Professor, Richard A. Rula of Civil and Environmental Engineering, Mississippi State Univ., Mississippi State, MS 39762 (corresponding author). ORCID: https://orcid.org/0000-0001-8883-4533. Email: farshid@cee.msstate.edu

Note. This manuscript was submitted on July 28, 2020; approved on September 11, 2021; published online on November 9, 2021. Discussion period open until April 9, 2022; separate discussions must be submitted for individual papers. This paper is part of the *International Journal of Geomechanics*, © ASCE, ISSN 1532-3641.

freeze-thaw can significantly fluctuate the temperature at the surface and within the top layer of soils. Temperature is shown to alter the microstructural characteristics (Goodman and Vahedifard 2019) and engineering properties (e.g., volume change, shear strength, stiffness, tensile strength) of unsaturated soils (e.g., Francois and Laloui 2008; Zhou and Ng 2016; McCartney et al. 2019; Vahedifard et al. 2019, 2020; Cao et al. 2021; Salimi et al. 2021a, b). Few studies have been performed to examine the effect of temperature on M_R . Jin et al. (1994) studied seasonal variations of M_R in granular soils. They used the experimentally measured data to develop an empirical model to capture changes in M_R with variation in suction and temperature by considering their effects on confining pressure. The Jin et al. (1994) model does not account for the effect of temperature on soil-water retention characteristics. Ng and Zhou (2014) conducted suctioncontrolled RLT tests on unsaturated silt samples varying different suctions and temperatures. They found that as the temperature increased from 20°C to 40°C, M_R decreased, and the difference was more pronounced at higher suctions. Miao et al. (2016) conducted RLT tests on unbound granular materials blended with asphalt pavement and virgin aggregates as the base course of pavement at varying temperature of 40°C, 22°C, 5°C, and -10°C. They observed a significant increase in M_R at the freezing temperature. They attempted to empirically capture the effect of temperature on M_R by varying the fitting parameters used in the Mechanistic-Empirical Pavement Design Guide (MEPDG) model (NCHRP 2004). Variation of resilient modulus with temperature can be attributed to the suction-dependency of M_R and the fact that suction itself is affected by changes in temperature. The temperature-dependency of suction is attributed to thermalinduced changes in the surface tension of the pore water, soil-water contact angle, soil fabric, water absorption potential, and pore size characteristics (Grant and Salehzadeh 1996; Romero et al. 2001; Vahedifard et al. 2018).

Soil-atmospheric interactions lead to frequent infiltration and evaporation processes in the unsaturated active zone above the water table, causing hydraulic hysteresis (drying and wetting cycles) in unsaturated subgrade soils. The hysteresis effects on the soil behavior are attributed to different mechanisms such as capillary condensation, geomaterial effects associated with pore size distribution, swelling and shrinkage, and contact angle hysteresis (Lu and Likos 2004). Hydraulic hysteresis considerably affects the soil-water retention curve (SWRC), in which the soil maintains a higher suction on the drying path compared with the wetting path at a given water content. Further, drying and wetting cycles can decrease the shear strength, increase the compressibility, alter the soil fabric, and cause the formation of cracks in unsaturated soil (e.g., Alonso et al. 2005; Tang et al. 2016; Esfandiari et al. 2021; Monghassem et al. 2021). Accordingly, variations in M_R are affected by drying and wetting cycles, proportional to changes in degree of saturation and matric suction along the primary and subsequent drying and wetting paths of the SWRC. Only a limited number of studies have examined the effect of hydraulic hysteresis on M_R . Furthermore, it has been shown that M_R has a higher value on the drying curve than the wetting curve in subgrades with considerable fines content (Khoury and Zaman 2004; Khoury et al. 2012), which can be attributed to the intrinsic relationship between M_R and the SWRC.

While the existing models are able to predict M_R at low suction with reasonable accuracy, their predictive capabilities significantly degrade at high suctions. Further, there is no M_R model in the literature that explicitly accounts for the effect of temperature, changes in deviatoric stress, and hydraulic hysteresis. To addresses the aforementioned limitations, this study aims to develop a generalized model capable of predicting M_R over a wide range of water content, suction, and temperature while accounting for the effects

of changes in deviatoric stress and hydraulic hysteresis. The model is validated against a total of 218 measured M_R reported in the literature across 14 different test sets of nine soils subjected to various levels of suction, deviatoric stress, and temperature. Furthermore, the predictive accuracy of the model is compared against four alternative models.

Background

Several predictive models have been proposed in the literature to capture the relation between M_R , stress levels, and suction (or water content). The existing models can be divided into three categories of semiempirical models, models incorporating suction through the concept of effective stress, and models using two independent stress state variables (Han and Vanapalli 2016). This section provides a brief overview of some of the existing models. Comprehensive details about the existing models are presented and critically reviewed in the literature (e.g., Puppala 2008; Han and Vanapalli 2016; Chu 2020).

Among the large number of semiempirical models, the MEPDG model (NCHRP 2004) has been extensively used in pavement design and can be represented as

$$M_R = k_1 P_a \left(\frac{\theta_b}{Pa}\right)^{k_2} \left(\frac{\tau_{oct}}{Pa} + 1\right)^{k_3} \tag{1}$$

where P_a = atmospheric pressure (~101.3 kPa); θ_b = bulk stress; τ_{oct} = octahedral shear stress; and k_1 to k_3 = fitting parameters. The MEPDG model determines M_R at the optimum moisture content (OMC). In the MEPDG model, κ_1 is proportional to Young's modulus and has a positive value, κ_2 incorporates the effect of bulk stress and shall be a positive value since an increase in the confining pressure increases M_R , and κ_3 is negative because increasing shear stress produces a softening effect on the material and reduces M_R . The MEPDG model predicts the resilient modulus of unbound and cohesive soil materials required for adequate structural performance of pavement layers. Several departments of transportation (DOTs) across the United States have created M_R databases for local soils with the intent of improving pavement designs and analyses (Nazzal and Mohammad 2010). The MEPDG (NCHRP 2004) intends to replace the AASHTO Guide for Design of Pavement Structures (AASHTO 1993) by requiring an in-depth analysis of pavements based on local traffic, climate and material conditions. The MEPDG suggests the following model to consider variation in water content:

$$\log\left(\frac{M_R}{M_{R,\text{OPT}}}\right) = a + \frac{b - a}{1 + \exp\left[\ln\left(-\frac{b}{a}\right) + k_m(S - S_{\text{OPT}})\right]}$$
(2)

where $M_{R,\mathrm{OPT}}$ = resilient modulus at OMC; S = degree of saturation; S_{OPT} = degree of saturation at OMC; $a = \min \log (M_R/M_{R,\mathrm{OPT}})$ (recommended to be -0.5934 for fine-grained soils); $b = \max \log (M_R/M_{R,\mathrm{OPT}})$ (recommended to be 0.4 for fine-grained soils); and k_m = fitting parameter recommended to be 6.13 and 6.82 for fine-grained and coarse-grained soils, respectively (Han and Vanapalli 2016).

The second group of models incorporates the effect of suction through the concept of effective stress. This approach allows them to consider the effects of both suction and degree of saturation on M_R . Following this concept, Yang et al. (2005) proposed the following equation to capture the effect of suction on degree of

saturation on M_R :

$$M_R = l_1 (\sigma_d + \chi \psi)^{l_2} \tag{3}$$

where ψ = suction; χ = Bishop's effective stress parameter; and l_1 and l_2 = fitting parameters. Liang et al. (2008) extended the MEPDG model and suggested

$$M_R = m_1 P_a \left(\frac{\theta_b + \chi \psi}{P_a}\right)^{m_2} \left(\frac{\tau_{\text{oct}}}{P_a} + 1\right)^{m_3} \tag{4}$$

where m_1 to m_3 = fitting parameters. The equation was developed based on RLT test results of fine-grained soils over the suction range of 150–380 kPa.

The third group employs suction as a stress state variable and incorporates its impact on the mechanical behavior of unsaturated subgrade soils independently. For instance, Cary and Zapata (2011) presented

$$M_R = n_1 P_a \left(\frac{\theta_{\text{net}} - 3\Delta u_{w-\text{sat}}}{P_a} \right)^{n_2} \left(\frac{\tau_{\text{oct}}}{P_a} + 1 \right)^{n_3} \left(\frac{\psi_0 - \Delta \psi}{P_a} + 1 \right)^{n_4}$$
 (5)

where $\theta_{\rm net} = \theta_b - 3u_a$, $\Delta u_{w-{\rm sat}} =$ the buildup of pore-water pressure under saturated condition; $\psi_0 =$ initial soil suction; $\Delta \psi =$ relative change of soil suction with respect to ψ_0 as a result of buildup of pore-water pressure under unsaturated conditions, in this case $\Delta u_{w-{\rm sat}} = 0$; and n_1 to $n_4 =$ fitting parameters, where n_1 , n_2 , and n_4 have positive values, and n_3 is negative. In this group, Han and Vanapalli (2015) proposed

$$\frac{M_R - M_{R,SAT}}{M_{R,OPT} - M_{R,SAT}} = \frac{\psi}{\psi_{OPT}} \left\{ \frac{\ln \left[2.718 + \left(\frac{\psi_{OPT}}{a_{FX}} \right)^{n_{FX}} \right]}{\ln \left[2.718 + \left(\frac{\psi}{a_{FX}} \right)^{n_{FX}} \right]} \right\}^{m_{FX}\xi}$$
(6)

where $M_{R,SAT}$ = resilient modulus at saturated condition; ψ_{OPT} = soil suction at OMC; a_{FX} , n_{FX} , and m_{FX} = fitting parameters of the Fredlund and Xing (1994) SWRC model; and ξ = model parameter. Han and Vanapalli (2015) evaluated the variation of ξ for nine sets of experimental data on six different soils and found values of ξ generally between 1 and 3.

Despite continuous advances in the development of M_R models, experimentally measured data (e.g., Banerjee et al. 2020a; Han and Vanapalli 2016; Freitas et al. 2020) show that the existing models are unable to accurately capture the changes in M_R when soil experiences high suctions. We hypothesize that this deficiency is due to

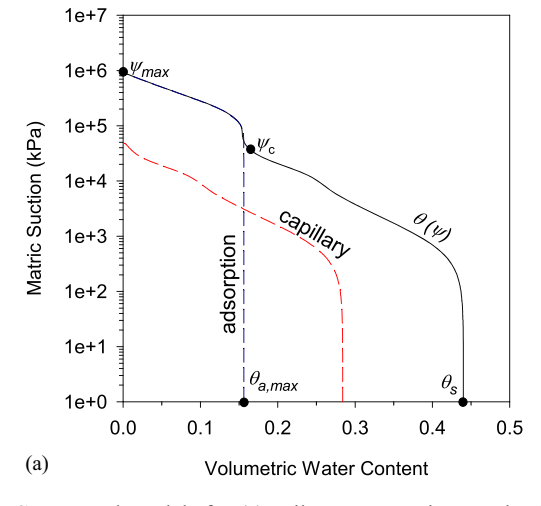
the failure of existing models to properly consider water retention mechanisms. Several studies have shown that the soil stiffness is strongly linked and controlled by the SWRC (e.g., Lu 2018; McCartney et al. 2019; Vahedifard et al. 2020). Further, the SWRC is not completely represented without independently considering both capillary and adsorption mechanisms (Tuller et al. 1999; Lu 2016). However, all existing M_R models consider capillarity as the only water retention mechanism causing M_R hardening. Since capillarity dominates in a low to medium range of suction (Tuller et al. 1999; Lu 2016), the existing models can predict M_R with reasonable accuracy only when suction varies within the capillarity range. However, the existing M_R models lose their predictive capability in high suctions in which adsorption is the dominant mechanism. The contribution of adsorption to water retention is overlooked in the current M_R models. In addition, the existing models do not explicitly consider the effect of temperature, changes in deviatoric stress, and hydraulic hysteresis. These shortcomings highlight the need for a generalized model, which can predict M_R over a wide range of water content (or suction), temperature, and stress conditions.

Model Development

Base Model: Effect of Water Content and Stress Level

In the first step, a base model is presented to determine M_R as a function of water content and stress level. The model is built upon the concept that variation in M_R with water content is controlled by two distinct water retention mechanisms of capillarity and adsorption. The water content is linked to suction through a two-part SWRC model proposed by Lu (2016) [Fig. 1(a)] that separately accounts for capillary and adsorption. Each part is incorporated in the development of the base model to independently capture changes in M_R with water content under capillary and adsorption mechanisms [Fig. 1(b)]. This feature allows the proposed model to accurately represent the characteristics of M_R over the entire range of suctions. It is noted that a similar approach was previously used by Lu (2018) to develop a two-part model for characterizing Young's modulus of unsaturated soils.

Most of the existing SWRC models are developed based on the cylindrical capillarity mechanism, ignoring the role of surface area and adsorbed water films in water retention (Tuller et al. 1999).



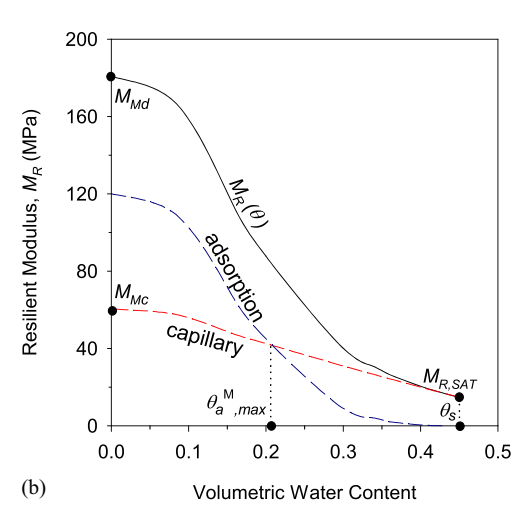


Fig. 1. Conceptual models for (a) soil-water retention mechanisms; and (b) resilient modulus, M_R , versus soil water content.

However, experimental and theoretical evidences display the existence of a second water retention mechanism in unsaturated porous media referred to as adsorption (e.g., Nitao and Bear 1996). Upon drying, the mechanism dominating soil-water interactions transitions from capillarity to adsorption. Capillary is the dominant mechanism of water retention in the low to medium range of suction (Tuller et al. 1999; Lu 2016). In the capillary zone (low to medium suctions), the soil particles are coated with thick films of free water and the surface tension controls interparticle bonding forces termed capillary forces. As the soil desaturates further (high suctions), the adsorption mechanism prevails in which thick water films no longer exist and water is stored in the form of thin liquid films adsorbed on the soil surface through physicochemical forces such as Van der Waals attraction, electrical double-layer repulsion, exchangeable cations, and surface hydroxyls forces (Lu 2016). Adsorption is mainly linked to the soil specific surface area and can have a considerable impact on the hydromechanical behavior of fine-grained soils in high suctions (Zhang and Lu 2020).

Nitao and Bear (1996) pointed out that the major problem with most of the SWRC models such as the van Genuchten (1980) model and the Fredlund and Xing (1994) model is their inability to distinguish between capillary and adsorptive forces. To address this issue, Tuller et al. (1999) proposed a SWRC model by considering both mechanisms of water retention in a porous media. More recently, Lu (2016) proposed a new SWRC model that distinguished adsorption and capillary water mechanisms and included additional important physical features such as cavitation and the highest matric suction. In this study, the Lu (2016) SWRC model is used and briefly described as follows.

Volumetric soil water content $\theta(\psi)$ at any given suction ψ comprises adsorption water content (θ_a) and capillary water content (θ_c) as

$$\theta(\psi) = \theta_a(\psi) + \theta_c(\psi) \tag{7}$$

For suctions greater than the cavitation pressure, soil water exists in adsorptive form, whereas both capillary and adsorption water coexist below the cavitation pressure. The adsorption water content can be defined as (Lu 2016)

$$\theta_a(\psi) = \theta_{a,\text{max}} \left\{ 1 - \left[\exp\left(-\frac{\psi_{\text{max}} + \psi}{\psi} \right) \right]^m \right\}$$
 (8)

where $\theta_{a,\text{max}} = \text{maximum}$ adsorption water content; $\psi_{\text{max}} = \text{maximum}$ suction; and m = parameter reflecting adsorption strength. Building upon the van Genuchten (1980) model, the capillary water content is defined as (Lu 2016)

$$\theta_c(\psi) = \frac{1}{2} \left[1 - \text{erf}\left(\sqrt{2} \frac{\psi - \psi_c}{\psi_c}\right) \right] \times \left[\theta_s - \theta_a(\psi)\right] \times \left[1 + (\alpha \psi)^n\right]^{((1/n) - 1)}$$
(9)

where erf () = error function (Mathews and Walker 1970); θ_s = saturated volumetric water content; α = fitting parameter related to air entry suction; n = related to pore size distribution; and ψ_c = mean cavitation pressure. It is noted that void ratio can have a considerable effect on the SWRC, particularly for compressible soils (e.g., Tarantino 2009; Pasha et al. 2017). For simplicity, however, we did not consider the effect of void ratio on the SWRC in this study.

Several studies have pointed to a direct correlation between water content (or suction) and M_R . Suction and resilient modulus are connected via soil-water content, both increase as the soil-water content decreases and both decrease as the soil moves toward saturation. Considering this observation, several studies have employed the SWRC as a tool to incorporate the effect of suction in predictive M_R models (e.g., Yang et al. 2005; Liang et al. 2008;

Sahin et al. 2013). It has been shown that M_R gradually increases as the soil starts to desaturate. This trend is followed by a sharp transition in M_R when adsorptive water retention begins to dominate, and M_R reaches its highest value when the soil is completely dry. This trend is quite similar to the rate by which suction changes with variation in soil-water content when either capillarity or adsorption is the dominant mechanism of water retention. This tendency has also been observed in elastic modulus and small strain shear modulus (e.g., Dong and Lu 2016; Lu 2018; Zhang and Lu 2020)

Based on the aforementioned observations, this study suggests a two-part model for M_R summing capillary and adsorptive parts as

$$M_R = M_{R,c}(\theta) + M_{R,a}(\theta) \tag{10}$$

where $M_{R,c}(\theta)$ and $M_{R,a}(\theta)$ = capillary and adsorptive parts, respectively, of the overall M_R . Fig. 1(b) schematically illustrates different components of the proposed model. Adopting a power function, $M_{R,c}(\theta)$ is expressed as

$$M_{R,c}(\theta) = (M_{R,SAT} - M_{Mc}) \left(\frac{\theta}{\theta_s}\right)^{m_M} + M_{Mc}$$
 (11)

where M_{Mc} = maximum M_R due to capillary at the dry state; and m_M = fitting parameter controlling the rate of M_R hardening in the capillary zone. Lu and Kaya (2014) employed a similar power function to model the hardening of Young's modulus due to capillary.

As discussed previously, in the range between a specific volumetric water content $(\theta_{a,\max}^m)$ and the point in which the soil is completely dry, adsorption becomes the dominant mechanism controlling M_R . In fine-grained soils, $\theta_{a,\max}^m$ has higher values, compared with coarse-grained soils, as the adsorption contribution to water retention is more pronounced in such soils. To capture this trend mathematically, $M_{R,a}(\theta)$ is defined as

$$M_{R,a}(\theta) = -r\theta + (M_{Md} - M_{Mc}) \tag{12}$$

where M_{Md} = maximum M_R at dry state; and r = rate of adsorptive hardening defined as

$$r = \frac{(M_{Md} - M_{Mc})\theta}{2\theta_{a,\max}^m}$$
 (13)

The Gaussian normal distribution with a standard deviation of $\theta_{a,\max}^m/2$ is applied to Eq. (12) to ensure a smooth transition between capillarity and adsorption as

$$M_{R,a}(\theta) = \frac{1}{2} \left[1 - \operatorname{erf}\left(\frac{2(\theta - \theta_{a,\text{max}}^{m})}{\theta_{a,\text{max}}^{m}}\right) \right] \times \left[-\frac{(M_{Md} - M_{Mc})\theta}{2\theta_{a,\text{max}}^{m}} + (M_{Md} - M_{Mc}) \right]$$
(14)

Effect of Deviatoric Stress

At a given confining pressure and suction, M_R decreases as σ_d increases, a trend that can be explained through the stress–strain behavior of unsaturated soils (e.g., Yao et al. 2018). In low values of σ_d , induced strains in subgrade soil are in the elastic range and increase proportionally as σ_d increases. However, beyond the yield strength, strains include both recoverable elastic strains (ε_p) and permanent plastic strains (ε_p). As σ_d increases, the ratio of ε_r to ε_p increases and, subsequently, σ_d/ε_r or M_R decreases. The effect of σ_d on M_R is more pronounced at higher suctions (Banerjee et al. 2020a, b). The behavior is attributed to the higher shear

strength of soil in higher suctions combined with its ability to noticeably lower strains especially at lower magnitudes of σ_d . Considering these observations, the current study suggests the following equation to account for the effect of changes in σ_d on M_R :

$$(M_R)_2 = (M_R)_1 \times \left[\frac{(\sigma_d)_1}{(\sigma_d)_2} \right]^{(\theta_s - \theta)^k}$$
 (15)

where $(M_R)_2$ = resilient modulus corresponding to the new deviatoric stress, $(\sigma_d)_2$; $(M_R)_1$ = measured resilient modulus at the reference deviatoric stress $(\sigma_d)_1$; and k = fitting parameter with a positive value incorporating the effect of volumetric water content and soil type. The k parameter is used in the formulation to represent the ratio of $(M_R)_2/(M_R)_1$ as a power function of $(\sigma_d)_1/(\sigma_d)_2$ and to capture the rate of increase in resilient modulus as the soil moves toward dryer states [Fig. 2(a)]. A similar trend has been reported in several of previous studies (e.g., Gupta et al. 2007; Zhang et al. 2021). This difference is more pronounced in fine-grained soils where M_R is significantly affected by water content, leading to higher k values in such soils. As will be discussed in more detail in the following sections, we found k to generally have a value between 0.8 and 1.5 depending upon the soil type.

Effect of Temperature

We account for the impact of temperature on M_R by employing a temperature-dependent SWRC proposed by Vahedifard et al. (2018), which separately incorporates the effect of temperature on adsorption and capillarity. The temperature-dependent SWRC model used in this study is extensively validated by Vahedifard et al. (2018) and Thota et al. (2020) for different soil types tested under various temperatures. Experimental studies show that, under a constant water content, increasing temperature will decrease the suction, inducing a downward shift in the SWRC (e.g., Schneider and Goss 2011; McCartney et al. 2019). Changes in temperature affect the surface tension of the pore water, soil-water contact angle, soil fabric, and water absorption potential (e.g., Grant and Salehzadeh 1996; Salager et al. 2007; Zhou et al. 2014; Vahedifard et al. 2018). In low degrees of saturation, changes in temperature affect the soil fabric and its adsorption capacity (e.g., Romero et al. 2001). Within the capillary regime, however, increasing temperature reduces surface tension and expands the trapped air bubbles, which will lead to a reduction of soil suction.

The Freundlich model (Ponec et al. 1974; Jeppu and Clement 2012) can be used to describe the amount of adsorbate (liquid) on a flat adsorbent (solid) in thermodynamic energy equilibrium

with the ambient adsorbate (in vapor phase) as

$$\theta_a = \theta_{a,\text{max}} (RH)^{1/m} \tag{16}$$

where RH = relative humidity. As defined previously, m = adsorption strength. Revil and Lu (2013) recast Eq. (16) by imposing the Kelvin–Laplace equation as

$$\theta_a = \theta_{a,\text{max}} \left[\exp\left(-\frac{M_w \psi}{RT}\right) \right]^{1/m} \tag{17}$$

where $M_w = \text{molar}$ volume of water and is equal to $1.8 \times 10^{-5} \text{ m}^3 \text{ mol}^{-1}$; R = universal gas constant and is equal to $8.314 \text{ J mol}^{-1} \text{ K}^{-1}$; and T = temperature in Kelvin. A temperature-dependent equation for suction can be expressed as (Grant and Salehzadeh 1996)

$$\psi = \psi_{T_r} \left(\frac{\beta + T}{\beta_{T_r} + T_r} \right) \tag{18}$$

where T_r = reference temperature; ψ_{T_r} = suction at the reference temperature; and β and β_{T_r} = regression parameters defined in terms of surface tension, contact angle, and enthalpy of immersion with respect to new and the reference temperature. The parameter β is determined as (Grant and Salehzadeh 1996)

$$\beta = \frac{-\Delta h_T T_r}{\Delta h_{T_r} + c(\cos \alpha')_{T_r} + d(\cos \alpha')_{T_r} T_r}$$
(19)

where α' = soil-water contact angle; and Δh_T = enthalpy of immersion per unit area; c and d = fitting parameters that can be estimated from the work of Dorsey (1940) and Haar et al. (1984) to be $c = 0.11766 \text{ N m}^{-1}$ and $d = -0.0001535 \text{ N m}^{-1}$ K. The temperature dependency of the enthalpy can be captured as (Watson 1943)

$$\Delta h_T = \Delta h_{T_r} \left(\frac{1 - T_r}{1 - T} \right)^{0.38} \tag{20}$$

where Δh_{T_r} = enthalpy of immersion per unit area at the reference temperature. The temperature-dependent soil-water contact angle is given as (Grant and Salehzadeh 1996)

$$\cos \alpha' = \frac{-\Delta h + TC_1}{c + dT} \tag{21}$$

where C_1 = constant defined as (Grant and Salehzadeh 1996)

$$\frac{\Delta h_{T_r} + c(\cos\alpha')_{T_r} + d(\cos\alpha')_{T_r} T_r}{T_r}$$
 (22)

Eqs. (17) and (18) can be incorporated into Eqs. (8) and (9) to account for the effect of temperature on adsorbed and capillary water. The need for only one extra parameter, Δh_{T_r} , to account

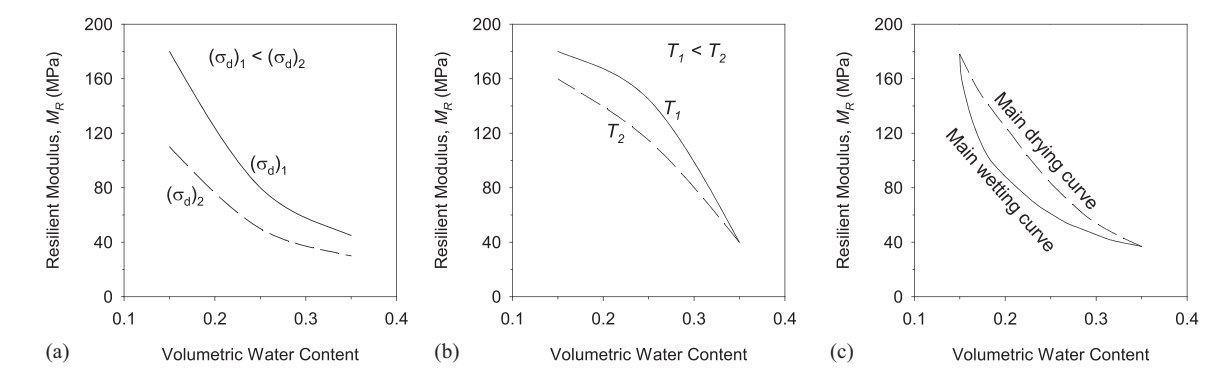


Fig. 2. Variation of resilient modulus versus water content: (a) effect of deviatoric stress; (b) effect of temperature; and (c) effect of hydraulic hysteresis.

for temperature is an important advantage of the proposed temperature-dependent formulation. The enthalpy can be obtained through experimental measurements or by using differential enthalpy of adsorption of the vapor (Everett 1972). Measured Δh_{T_r} values for different soil types are presented in Grant and Salehzadeh (1996) and Vahedifard et al. (2020). For instance, the enthalpy values of -285 and -516 mJ/m³ are reported for silty loam and sandy loam, respectively, at $T=25^{\circ}$ C (Grant and Salehzadeh 1996).

Fig. 2(b) schematically illustrates the impact of temperature on M_R . As shown, M_R decreases as the temperature increases. Thermalinduced changes in M_R become more significant as the soil volumetric water content reaches low values (near residual saturation). As discussed previously, there is a direct relationship between the suction (or the SWRC) and the soil stiffness (or M_R). At a constant water content, elevating temperature decreases suction, which leads to a lower contribution of suction to soil stiffness. This trend results in subgrade soil having lower M_R in higher temperatures. When the soil moves toward saturation, suction decreases significantly, and the effect of temperature becomes less pronounced (Ng and Zhou 2014).

Effect of Hydraulic Hysteresis

Experimentally measured M_R values reveal a path-dependent behavior, particularly in fine-grained soils, with a higher value of M_R along the drying path compared with the wetting path (e.g., Khoury et al. 2012). However, the majority of existing M_R models do not incorporate the effect of hydraulic hysteresis. Higher suctions are developed when the soil is dried in comparison with when it is wetted, which leads to higher effective stress and eventually higher values of M_R [Fig. 2(c)]. The effect of hydraulic hysteresis on stiffness moduli in unsaturated soils can be attributed to suction-induced hardening (e.g., Khosravi and McCartney 2012), which is due to the irrecoverable energy consumed during desaturation (Esfandiari et al. 2021; Monghassem et al. 2021). Since the area confined between the drying and wetting SWRCs represents the irrecoverable energy in a hydraulic hysteresis, we propose the following equation to capture the effect of hysteresis on M_R along the main drying and wetting paths:

$$(M_R)_W = (M_R)_D \times \left[\frac{\psi_W(\theta)}{\psi_D(\theta)} \right]^{k_h}$$
 (23)

where $(M_R)_W$ = resilient modulus along the main wetting path; $(M_R)_D$ = resilient modulus along the main drying path; $\psi_W(\theta)$

and $\psi_D(\theta)$ = suctions corresponding to the specific volumetric water content along the wetting and drying paths, respectively; and k_h = fitting parameter considering the soil type. In a fully saturated or dry condition, where the soil has the same suction on both drying and wetting paths, the ratio of $\psi_W(\theta)/\psi_D(\theta)$ is equal to 1 and $(M_R)_W = (M_R)_D$ (Khoury et al. 2012). In water contents in between, however, $(M_R)_W/(M_R)_D$ can be described by a power law $(\psi_W(\theta)/\psi_D(\theta))^{k_h}$. Fine-grained soils that exhibit with a greater difference in suction developed on drying and wetting paths at a given water content, and consequently greater a difference of M_R on each path, have higher values of k_h .

Validation and Comparison

A total of 14 sets (218 testing data points) of experimentally measured results using RLT tests on nine different compacted fine-grained subgrade soils are collected from the literature and used to validate the performance of the proposed model. Table 1 summarizes the 14 data sets used in this section along with the corresponding SWRC fitting parameters. For each set, the original reference reporting the RLT test results is provided in Table 1. Soils 11 and 12 share the same SWRC with Soils 3 and 5 but since they were used in different studies and tested under different conditions, they are presented as different sets. Table 2 lists the parameters of the proposed M_R model for these 14 sets.

The coefficient of determination (R^2) and the root mean square error (RMSE) are used in this study to statistically examine and compare the predictive accuracy of the proposed model and four alternative models. For each set, RMSE is calculated as

$$RMSE = \sqrt{\frac{\sum_{i=1}^{n} (\widehat{y}_i - y_i)^2}{N}}$$
 (24)

where \hat{y} and y = measured and predicted values, respectively; and N = total number of samples.

Validation of Base Model

The measured data from RLT tests on Soils 1–6 (Table 1) are used to validate the base model. Further, the results are compared against those predicted using four alternative models proposed by MEPDG (NCHRP 2004), Liang et al. (2008), Cary and Zapata (2011), and

Table 1. SWRC parameters of subgrade soils reported in the literature used for validation in this study

Soil no.	Soil ID	$\alpha (\text{kPa}^{-1})$	n	m	$\psi_{\rm max}$ (kPa)	ψ_c (kPa)	$\theta_{a ext{max}}$	θ_s	Reference
1	Silt	0.080	1.39	0.05	7.5×10^{5}	6.0×10^{3}	0.04	0.38	Banerjee et al. (2020a)
2	Clay	0.001	1.38	0.30	3.0×10^{6}	1.4×10^{5}	0.09	0.45	Banerjee et al. (2020a)
3	Red Wing	0.020	1.42	1.00	2.0×10^{5}	2.5×10^{5}	0.02	0.31	Sawangsuriya et al. (2009)
4	Duluth TH23 Slopes	0.006	1.28	2.10	2.0×10^{5}	8.0×10^{3}	0.17	0.49	Sawangsuriya et al. (2009)
5	MnRoad	0.004	1.41	0.98	1.5×10^{5}	2.5×10^{4}	0.07	0.33	Sawangsuriya et al. (2009)
6	Red Lake Falls	0.005	1.31	0.75	2.0×10^{5}	2.5×10^4	0.08	0.38	Sawangsuriya et al. (2009)
7	CLS-RC 85%	0.068	1.23	0.30	1.2×10^{6}	2.5×10^{4}	0.01	0.26	Zhang et al. (2021)
8	CLS-RC 90%	0.050	1.34	0.42	1.2×10^{6}	2.5×10^{4}	0.03	0.24	Zhang et al. (2021)
9	CLS-RC 95%	0.090	1.19	0.42	1.2×10^{6}	2.5×10^4	0.01	0.22	Zhang et al. (2021)
10	CLS-RC 100%	0.365	1.12	0.42	1.2×10^{6}	2.5×10^{4}	0.01	0.21	Zhang et al. (2021)
11	Red Winga-G	0.020	1.42	1.00	2.0×10^{5}	2.5×10^{4}	0.02	0.31	Gupta et al. (2007)
12	MnRoad ^a -G	0.004	1.41	0.98	1.5×10^{5}	2.5×10^{4}	0.07	0.33	Gupta et al. (2007)
13	Hong Kong silt	0.020	1.43	2.16	1.0×10^{5}	6.6×10^{3}	0.01	0.35	Ng and Zhou (2014)
14	Renfrow-D ^b	0.002	1.18	2.00	5.2×10^4	1.2×10^{4}	0.01	0.34	Zaman and Khoury (2007)
	Renfrow-W ^b	0.006	1.17	2.00	5.2×10^4	2.5×10^4	0.01	0.33	• ` ` ´

^aRed Wing-G and MnRoad-G have the same SWRC as Red Wing and MnRoad. Since they were tested in two different studies under different conditions, they are represented as different sets.

^bFor this soil, values shown in top and bottom rows represent the fitting parameters with respect to main drying path and main wetting path, respectively.

Han and Vanapalli (2015). Tables 2 and 3 present the parameters of the proposed model and the four alternative models, respectively, for each soil used in this section. For the alternative models, we used the measured data for each soil along with the least-squares optimization technique to obtain the fitting parameters needed for the functional form proposed in the original reference for each model (Table 3). Whenever available, we used the recommended value for each petameter as suggested in the original reference. Table 4 provides a comparison of the predictive accuracy (in terms of R^2 and RMSE) of the proposed model versus the four alternative models at ambient temperature. Figs. 3 and 4 depict the measured and predicted SWRC and M_R , respectively, for Soil 1 to Soil 6.

Banerjee et al. (2020a) conducted a series of RLT tests on finegrained soils (Soils 1 and 2) using axis-translation and vapor pressure techniques to evaluate the M_R of subgrade soils over their

Table 2. Parameters of the proposed model for subgrade soils used for validation

Soil no.	Soil ID	$\theta_{a\mathrm{max}}^{M}$	M_{Mc} (MPa)	M_{Md} (MPa)	$M_{R,\mathrm{SAT}}$ (MPa)	m _M (kPa)
1	Silt	0.12	204	785	46.6	0.60
2	Clay	0.21	70	223	14.5	0.84
3	Red Wing	0.12	107	115	30	3.23
4	Duluth TH23 Slopes	0.27	180	265	12	3.30
5	MnRoad	0.22	150	186	13	2.71
6	Red Lake Falls	0.10	130	140	12	4.07
7	CLS-RC 85%	0.09	120	500	97	0.22
8	CLS-RC 90%	0.08	180	550	120	0.89
9	CLS-RC 95%	0.09	185	650	125	0.77
10	CLS-RC 100%	0.08	190	680	139	1.08
11	Red Wing-G	0.15	67	207	33	2.98
12	MnRoad-G	0.13	200	205	15	0.24
13	Hong Kong Silt	0.18	96	100	27	7.35
14	Renfrow-D a	0.15	146	1,742	38	1.8
	Renfrow-W ^b	0.15	146	1,650	20	1.8

^aValues correspond to $\theta_b = 154.64$ kPa and $\tau_{\text{oct}} = 13.00$ kPa.

entire range of suction from a saturated to fully dry state. They used two different soil samples: a nonplastic silty soil obtained from a site in Denison Texas and a mixture of locally available sandy clay and sodium bentonite clay. Measured and predicted SWRC of these two soils are shown in Figs. 3(a and b). The suction-controlled tests were conducted under a confining pressure of 27.6 and a deviator stress of 41.4 kPa as per AASHTO T307-99 (AASHTO 2012) recommendation. They reported the saturated resilient modulus ($M_{R,SAT}$) of the silt and clay samples were 46.6 and 14.5 MPa, respectively. Figs. 4(a and b) show the measured values of M_R of the two soil samples corresponding to different soil water contents along with predicted values using four other models and the proposed model in this study.

Sawangsuriya et al. (2009) measured M_R values of Soil 3 to Soil 6 (Table 1) to define an empirical relationship between M_R and suction. They measured the drying SWRC of each soil using a pressure plate extractor. The measured data and fitted SWRC are present through Figs. 3(c-f). All specimens were initially saturated by permeation in a flexible wall permeameter and then gradually desaturated using the axis-translation technique in the suction cell until they reached the target suction value during the test. Based on NCHRP 1-28A (NCHRP 2003), a deviatoric stress of 41 kPa and a confining pressure of 14 kPa were applied to the specimens in order to measure their M_R values.

As seen in Fig. 4 and Table 4, the proposed model can predict the measured data over the entire range of water content with a very high accuracy ($R^2 = 99\%$). For all six soils examined, the predictive errors of the proposed model are significantly lower than the four alterative models. The superior performance of the proposed model is more pronounced in low water contents (high suctions). The superior performance at low water content can be attributed to the explicit consideration of capillarity and adsorption as main mechanisms responsible for hardening of M_R over the entire range of suction in the proposed model. The results clearly show that the other models fail to capture the subgrade behavior in this region. For instance, volumetric water content of 0.1 in MnRoad soil [Soil 5, Fig. 3(e)] corresponds to about 18 MPa suction, and

Table 3. Fitting parameters of four alternative models used for comparison for Soils 1-6

		ME	PDG [Eq.	(2)]	Liang et al. (2008) Cary and Zapata (2011) [Eq. (4)] [Eq. (5)]			Han and Vanapalli (2015) [Eq. (6)]										
Soil no.	Soil ID	k_m	$M_{R,\mathrm{OPT}}$	$S_{ m OPT}$	m_1	m_2	m_3	n_1	n_2	n_3	n_4	ξ	$M_{R,\mathrm{OPT}}$	$M_{R,\mathrm{SAT}}$	ψ_{OPT}	a_{FX}	n_{FX}	m_{FX}
1	Silt	6.12	87.1	0.65	1.06	1.21	-0.01	1.67	0.03	-1.96	0.28	3.21	87.1	45.0	36	18	0.80	1.0
2	Clay	7.12	26.2	0.83	0.07	0.71	-0.01	0.17	0.03	-1.73	0.31	2.31	26.2	14.8	1,750	2,100	0.88	1.0
3	Red Wing	3.65	56.0	0.77	0.58	1.65	-0.51	0.61	0.01	-1.64	0.40	2.25	56.0	28.0	58	76	0.77	1.3
4	Duluth TH23 Slopes	7.30	60.0	12	0.03	2.70	-0.60	0.35	0.01	-2.14	0.48	1.77	60.0	12.0	465	28,971	0.59	7.7
5	MnRoad	6.54	57.0	0.77	0.33	0.69	-0.10	0.52	0.01	-1.67	0.28	3.21	57.0	10.0	165	980	0.67	1.5
6	Red Lake Falls	25.41	57.0	0.88	0.24	1.24	-0.10	0.41	0.01	-1.77	0.47	5.25	57.0	11.0	60	1,678	0.59	2.0

Table 4. Evaluation of prediction accuracy of the proposed model versus four alternative models at ambient temperature

		MEPDG (NCHRP 20		Liang et al. (2008)		Cary and Za (2011)	pata	Han and Vana (2015)	apalli	Proposed model		
Soil no.	Soil ID	RMSE (MPa)	R^2	RMSE (MPa)	R^2	RMSE (MPa)	R^2	RMSE (MPa)	R^2	RMSE (MPa)	R^2	
1	Silt	243.0	0.88	109.0	0.91	79.0	0.95	133.0	0.88	6.4	0.99	
2	Clay	21.1	0.92	9.2	0.98	8.6	0.98	18.5	0.95	2.6	0.99	
3	Red Wing	10.9	0.94	10.5	0.92	11.6	0.89	10.5	0.95	3.2	0.98	
4	Duluth TH23 Slopes	34.3	0.97	1,018.0	0.96	12.4	0.98	10.0	0.99	5.2	0.99	
5	MnRoad	26.8	0.96	19.0	0.94	20.0	0.93	12.8	0.98	9.7	0.98	
6	Red Lake Falls	16.7	0.98	21.6	0.87	22.9	0.85	22.2	0.99	14.0	0.95	

^bValues correspond to $\theta_b = 83.00$ kPa and $\tau_{\text{oct}} = 19.30$ kPa.

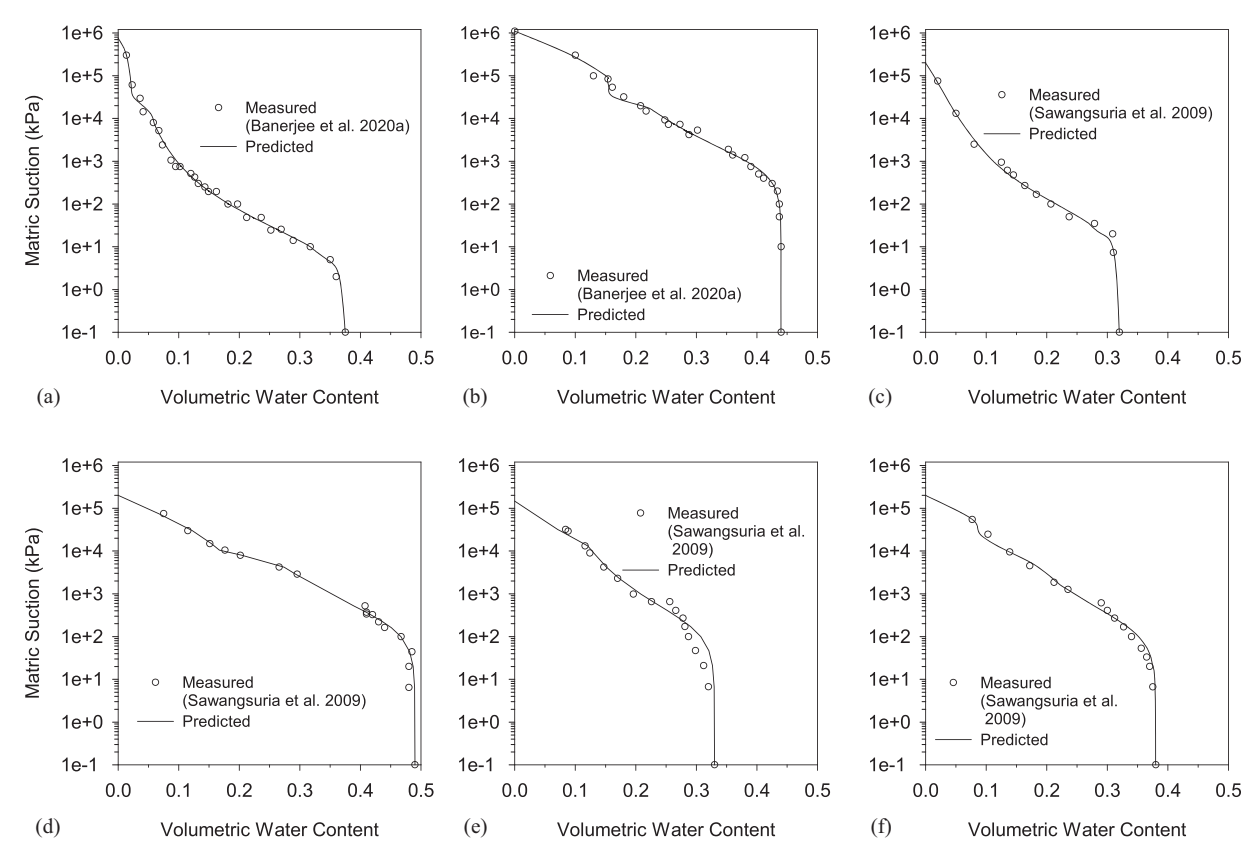


Fig. 3. Measured and predicted SWRC for different soils: (a) silt (Soil 1); (b) clay (Soil 2); (c) Red Wing (Soil 3); (d) Duluth TH23 Slopes (Soil 4); (e) MnRoad (Soil 5); and (f) Red Lake Falls (Soil 6).

the soil behavior in this suction range cannot be fully captured by considering only capillary mechanism. The absence of the adsorption mechanism in the existing models explains why they accurately predict M_R at high degrees of saturations but fail to predict M_R in dryer conditions.

Among the four alternative models that were examined, the MEPDG model shows the lowest accuracy. It has a reasonable performance when the soil is near saturation but significantly loses its accuracy as the soil moves toward dryer conditions. The models by Liang et al. (2008) and Cary and Zapata (2011) resulted in close M_R values for different volumetric water contents. This comparable performance can be attributed to the similar functional forms of the two models, which are both extensions of the MEPDG model, except that the Liang et al. (2008) model employs an effective stress approach while the Cary and Zapata (2011) model is based on a stress state approach. Both models perform well when the soil suction is low but lose their predictive accuracy as the suction increases. Between the four alternative models, the Han and Vanapalli (2015) model exhibits the highest accuracy, especially when the suction is in the range of 0-1,000 kPa. However, the model predictive capability diminishes in higher suction. This poor performance can be seen in Fig. 4(a) for $\theta = 0.02 - 0.10$ corresponding to suctions of 100,000–1,000 kPa. Further, in high suctions, the parameter ξ no longer has the unique value of 2, which was originally suggested by Han and Vanapalli (2015).

Unlike the majority of existing models, the proposed model takes the water content as the direct input instead of suction. This feature makes the model more suitable for practical applications, as measuring the water content in field conditions is much more common and convenient than measuring suction. Another point that can be learned from Figs. 3 and 4 is that $\theta_{a,\max}$ and $\theta_{a,\max}^M$ do

not share the same value, meaning that the boundary between capillary and adsorption mechanisms is different for water retention and M_R hardening. A similar behavior was previously observed for elastic modulus (Lu 2018).

Validation Considering Changes in Deviatoric Stress

Testing results for Soils 7–12 are used to evaluate the proposed model considering the effects of deviatoric stress. Experimentally measured results for Soil 7 through Soil 10 are reported by Zhang et al. (2021). Figs. 5 and 6 show the measured SWRCs and M_R of Soils 7 through 10 reported by Zhang et al. (2021) versus those predicted using the proposed formulation in this study. The measured M_R results for Soil 11 and Soil 12 are obtained from Gupta et al. (2007) and compared with those from the proposed model in Fig. 7. Table 5 presents R^2 and RMSE of the proposed model while considering the deviatoric stress effect for Soils 7–12.

For Soils 7–10, Zhang et al. (2021) used RLT tests and pressure plate techniques to study the effect of σ_d , relative compaction (RC), and suction on M_R . The tested soil was classified as a sandy low plasticity clay (CLS). The soil samples were compacted at a RC of 85%, 90%, 95%, and 100% and were tested under 80%, 100%, 120%, 140%, and 160% OMC. The SWRCs of the subgrade soil at four different compaction levels are shown in Fig. 5. The soil samples were subjected to 30 kPa confining pressure and σ_d of 10, 20, 30, and 40 kPa. In this case, M_R values at 10 kPa deviatoric stress are considered as the reference points and M_R values at higher deviatoric stresses are predicted using Eq. (15).

Fig. 6 shows the measured and predicted M_R values for Soil 7 to Soil 10. A constraint was introduced during the regression analysis to force M_R to decrease continuously as the water content increases.

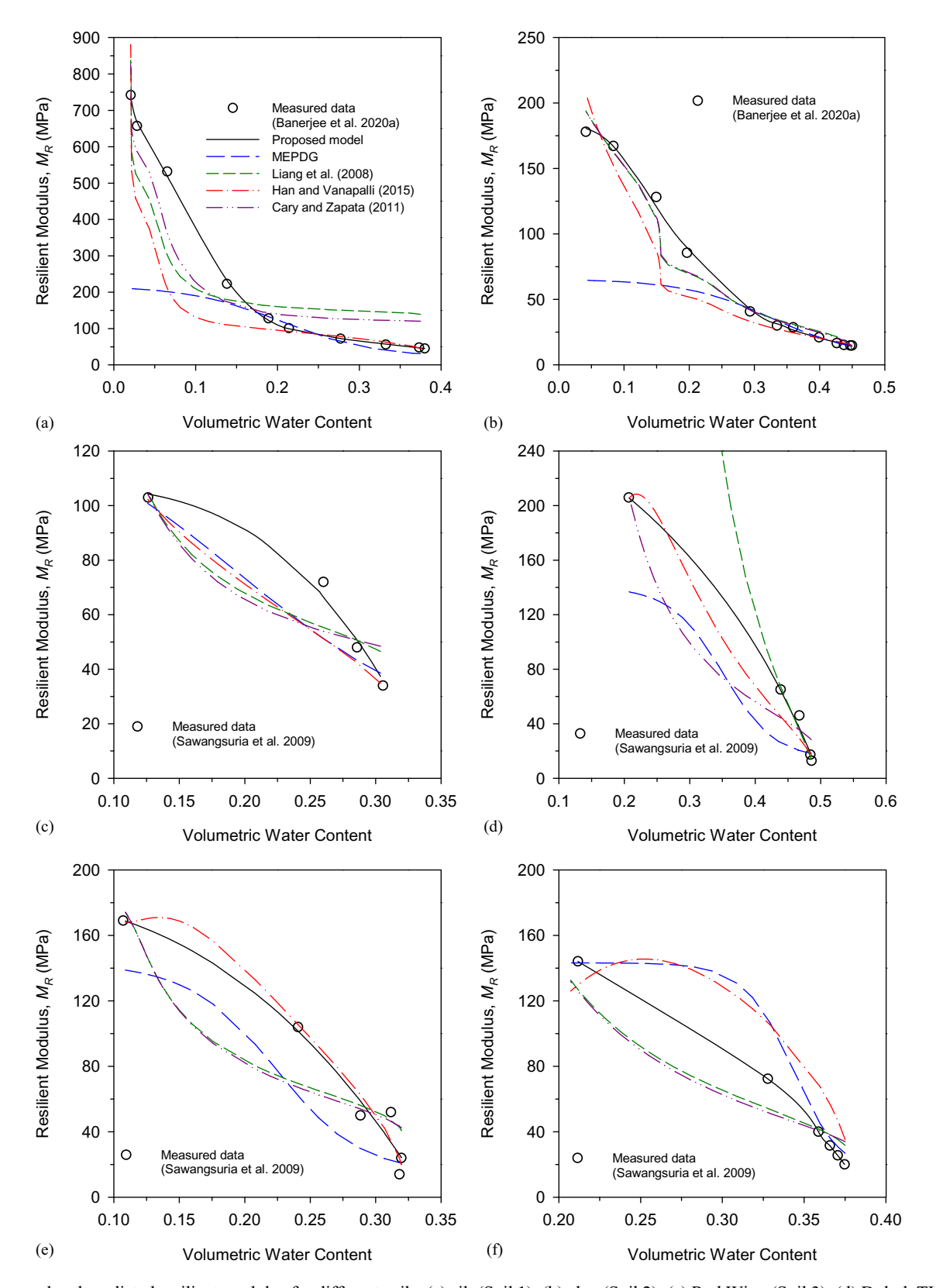


Fig. 4. Measured and predicted resilient modulus for different soils: (a) silt (Soil 1); (b) clay (Soil 2); (c) Red Wing (Soil 3); (d) Duluth TH23 Slopes (Soil 4); (e) MnRoad (Soil 5); and (f) Red Lake Falls (Soil 6).

As shown, M_R considerably decreases with an increase in σ_d . Furthermore, it is noted that the predicted M_R curves reach a plateau as the volumetric water content exceeds about 0.17, which in most cases reasonably capture the trend of the measured data. However, in a few cases, the measured M_R values suddenly drop at volumetric

water contents above 0.17, a trend that is not fully captured by the model. This can be due to limitations of the proposed model and/or possible errors in the laboratory testing measurements. Nevertheless, the overall trend of the measured data is reasonably captured using the proposed model. Table 5 presents the *RMSE* and R^2 of the

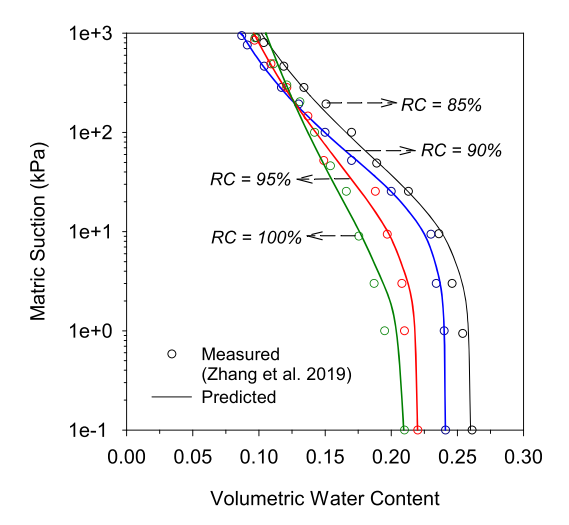


Fig. 5. Measured and predicted SWRC of sandy low plasticity clay with relative compaction of 85% (Soil 7), 90% (Soil 8), 95% (Soil 9), and 100% (Soil 10).

proposed model in predicting M_R while considering changes in σ_d . As shown, the proposed model captures the effect of σ_d on M_R with $R^2 = 99\%$ and a maximum of RMSE = 9.8 MPa. Gupta et al. (2007) tested Soil 11 (Red Wing-G) and Soil 12 (Mn-Road-G) to investigate the effect of σ_d and suction on their M_R values. The specimens were tested using triaxial testing apparatus equipped with the axistranslation technique and a thermal dissipation sensor to control and measure the suction. The soil specimens were compacted at OMC, saturated, and then desaturated to reach the desired level of suction before the test. Gupta et al. (2007) measured M_R of the soils for different suctions under $\sigma_d = 30$, 50, 70, and 100 kPa and the confining pressure of 14.5 kPa. The measured saturated resilient moduli of Red Wing and MnRoad samples were 33 and 15 MPa, respectively. In this study, M_R values at deviatoric stress of 50 and 30 kPa are considered as reference points for Soil 11 and Soil 12, respectively.

For all cases examined, M_R of the subgrade soils considerably decreases with an increase in σ_d . As shown in Figs. 6 and 7 as well as Table 5, the proposed model is able to capture the effect of σ_d on M_R with very high R^2 (>97%) and low *RMSE* values. It is also evident that k has a unique value for each level of compaction for each SWRC.

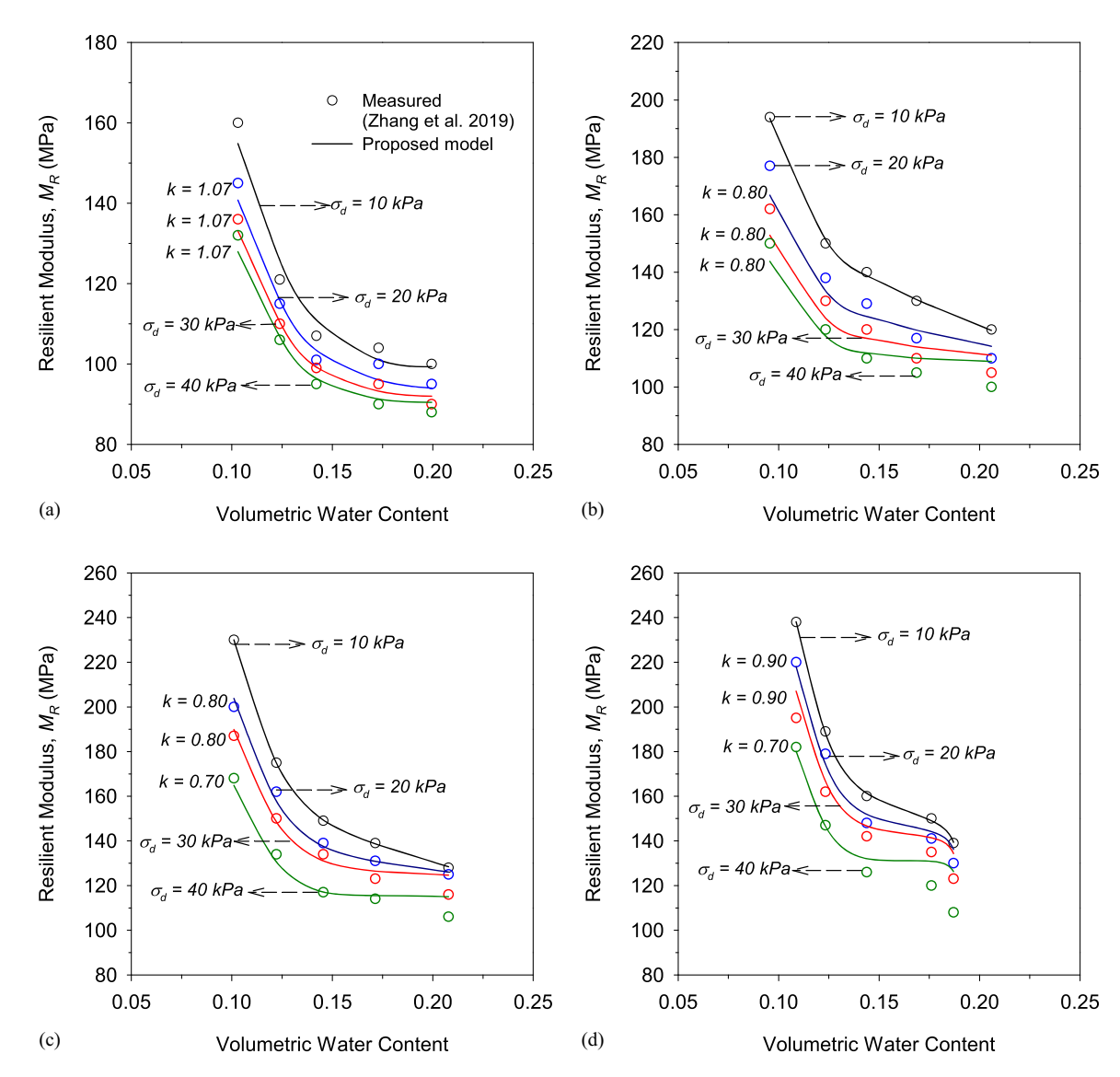


Fig. 6. Measured and predicted resilient modulus of sandy low plasticity clay at different relative compactions of (a) 85% (Soil 7); (b) 90% (Soil 8); (c) 95% (Soil 9); and (d) 100% (Soil 10).

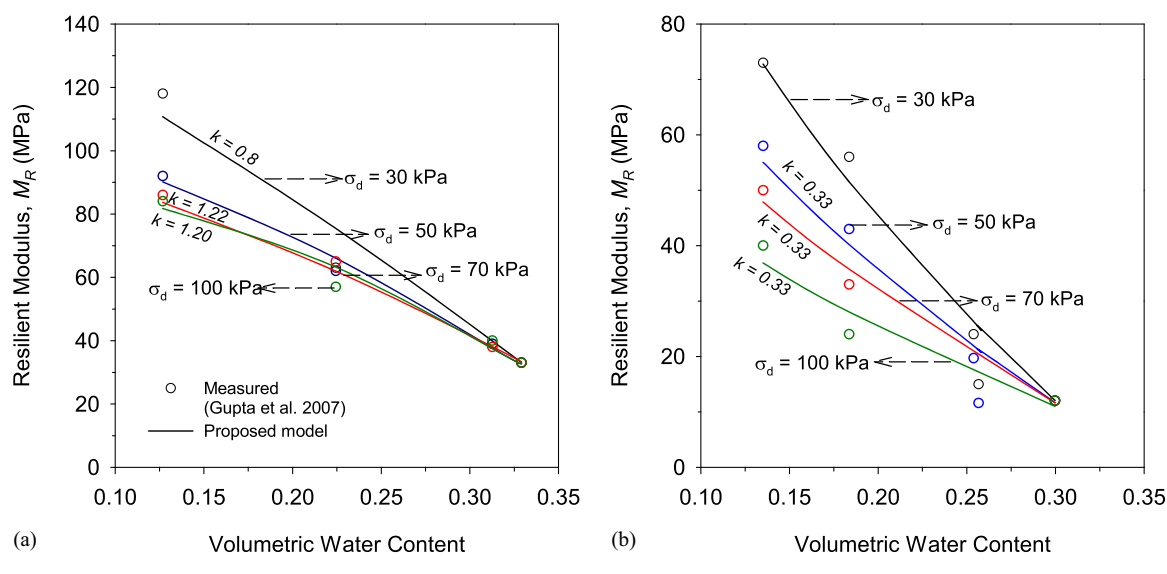


Fig. 7. Measured and predicted resilient modulus of (a) Red Wing-G (Soil 11); and (b) MnRoad-G (Soil 12).

Table 5. Evaluation of the proposed model considering deviatoric stress effect

			Proposed mo	odel
Soil no.	Soil ID	σ_d (kPa)	RMSE (MPa)	R^2
7	CLS-RC 85%	10	3.87	0.99
		20	2.87	0.99
		30	1.77	0.99
		40	2.32	0.99
8	CLS-RC 90%	10	3.72	0.99
		20	5.81	0.99
		30	6.00	0.99
		40	5.53	0.99
9	CLS-RC 95%	10	0.30	0.99
		20	2.68	0.99
		30	4.60	0.99
		40	4.57	0.99
10	CLS-RC 100%	10	3.22	0.99
		20	4.19	0.99
		30	8.47	0.99
		40	9.80	0.98
11	Red Wing-G	30	8.32	0.97
		50	2.33	0.99
		70	1.80	0.99
		100	3.54	0.98
12	MnRoad-G	30	5.17	0.98
		50	4.79	0.98
		70	2.03	0.99
		100	3.01	0.97

Validation at Elevated Temperature

Test results on Hong Kong silt (Soil 13, Table 1) reported by Ng and Zhou (2014) are used to evaluate the proposed model considering the effects of temperature on M_R . Ng and Zhou (2014) investigated the effect of suction and temperature on the cyclic behavior of Hong Kong silt. The soil specimens were compacted at an initial water content of 16.3% to reach the maximum dry unit weight of 17.3 kN/m³.

Ng and Zhou (2014) conducted seven suction- and temperature-controlled cyclic triaxial tests on the specimens at temperatures of 20°C and 40°C and suctions of 0, 30, and 60 kPa. Specimens initially had a suction of 95 kPa and then were gradually wetted to

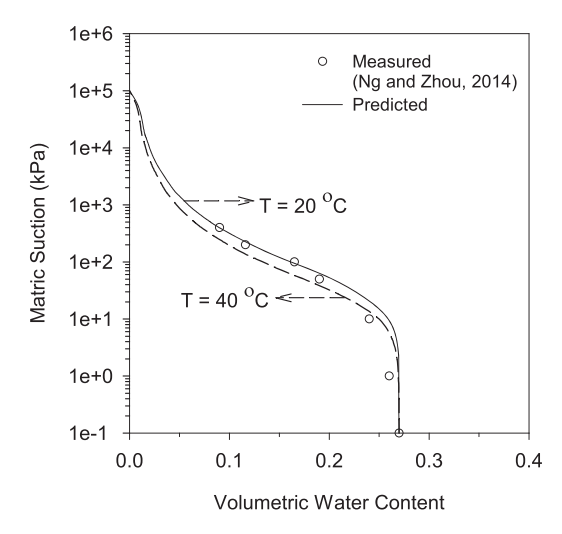


Fig. 8. Measured and predicted SWRC of Hong Kong silt (Soil 13).

reach suctions of 60, 30, and 0 kPa. Thus, the wetting path of the SWRC is used in this study (Fig. 8). For the tests carried out at elevated temperatures, the specimens were heated to 40°C. As thermal loading might induce excess pore-water pressure, 3–5 days were needed for dissipation of the generated pore-water pressure. Once suction and temperature equilibriums were reached, the specimens were tested under a confining pressure of 30 kPa and deviatoric stresses (σ_d) of 30, 40, 55, and 70 kPa. Ng and Zhou (2014) used a suction-controlled triaxial apparatus, which allowed independent control of suction and temperature. Pore-air pressure and pore-water pressure were controlled using the axis-translation technique, while a heating system consisted of a thermostat, a heater, and thermocouple was used to heat the specimen. While no measured SWRC data at 40°C were presented in Ng and Zhou (2014), the SWRC at 40°C is predicted using Eqs. (10) and (18) and employed in the current study to capture the effect of temperature. A value Δh_{T_c} of -516 mJ/m³ is used in the calculation, adopted from the value reported for a comparable silty soil by Grant and Salehzadeh (1996).

Fig. 9 shows a comparison between the measured and predicted M_R values for four different $\sigma_d s$. In the proposed solution, M_R at ambient temperature (20°C) has been used as a reference point to predict the M_R values at 40°C. As shown, M_R decreases with an

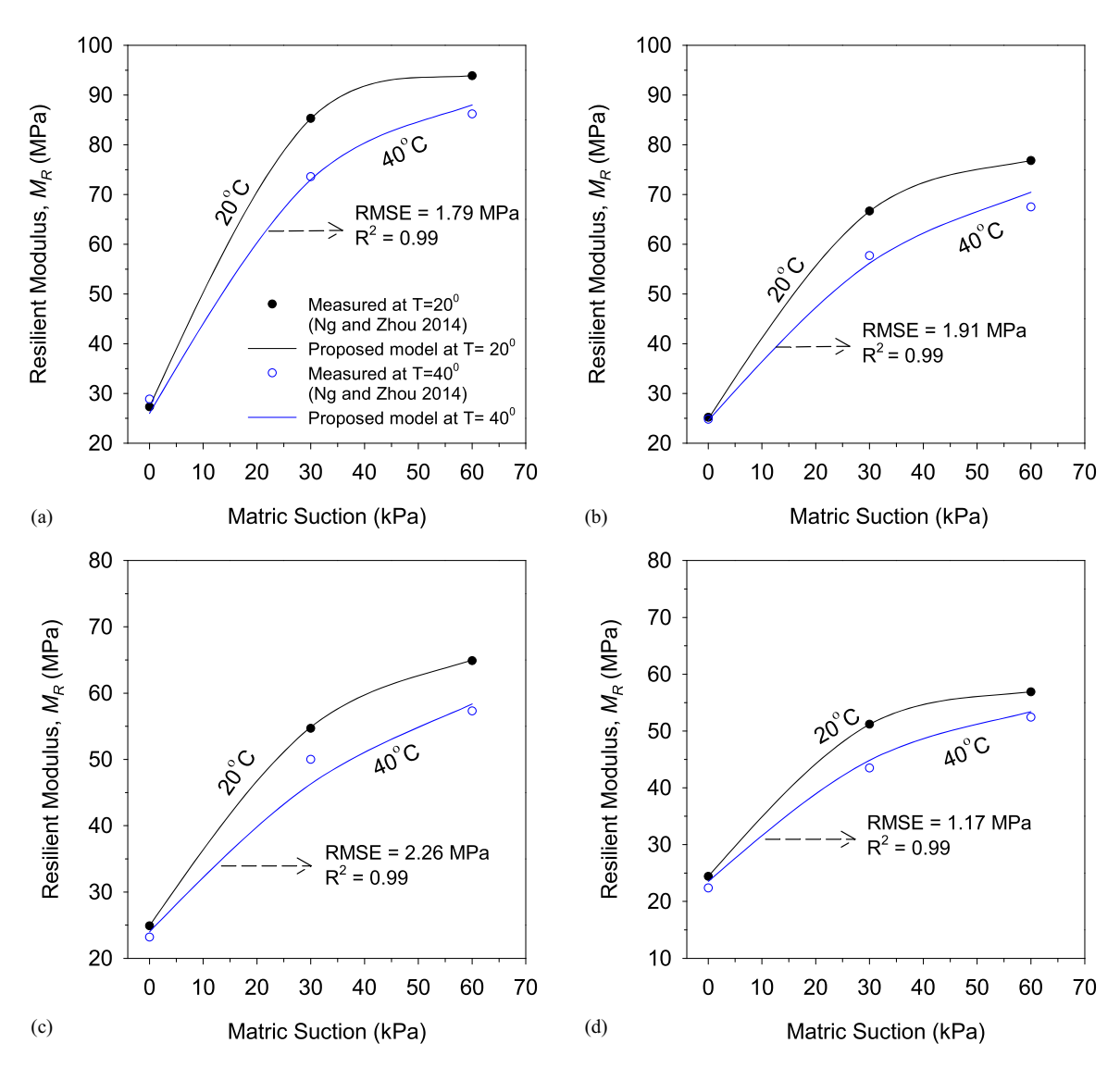


Fig. 9. Measured and predicted resilient modulus of Hong Kong silt (Soil 13) at different deviatoric stresses: (a) $\sigma_d = 30$ kPa; (b) $\sigma_d = 40$ kPa; (c) $\sigma_d = 55$ kPa; and (d) $\sigma_d = 70$ kPa.

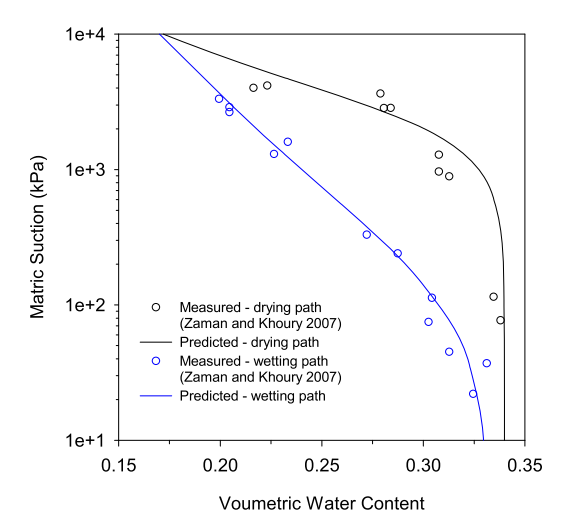


Fig. 10. Measured and predicted SWRC of Renfrow clay (Soil 14).

increase in temperature. For each set, Fig. 9 includes R^2 and RMSE of the proposed model considering the effect of temperature.

Results show the capability of the proposed model in capturing the effect of temperature on M_R .

Validation Considering Hydraulic Hysteresis

Test results on Renfrow soil (Soil 14, Table 1) reported by Khoury et al. (2012) are used to evaluate the proposed model for considering the effects of hydraulic hysteresis. Khoury et al. (2012) investigated the effect of hysteresis on resilient modulus of subgrade soil following two different paths: (1) drying—wetting—drying path, and (2) wetting—drying path. Since the proposed model in this paper captures the hysteresis effect along main drying and wetting paths, the measured data for Path (1) are used for validation in this section.

Khoury et al. (2012) conducted a total of 10 tests on Renfrow soil specimens. Renfrow soil is classified as inorganic clay of low to medium plasticity with liquid limit of 35 and plasticity index of 15. The maximum dry unit weight of 16.6 kN/m^3 at OMC of 16.5% was reported for the soil. Soil specimens were prepared at OMC in accordance with the laboratory procedure proposed by Khoury and Zaman (2004) to ensure a uniform distribution of moisture within the specimen. Khoury et al. (2012) established the starting point on an initial drying curve by conducting an M_R test on a specimen prepared at

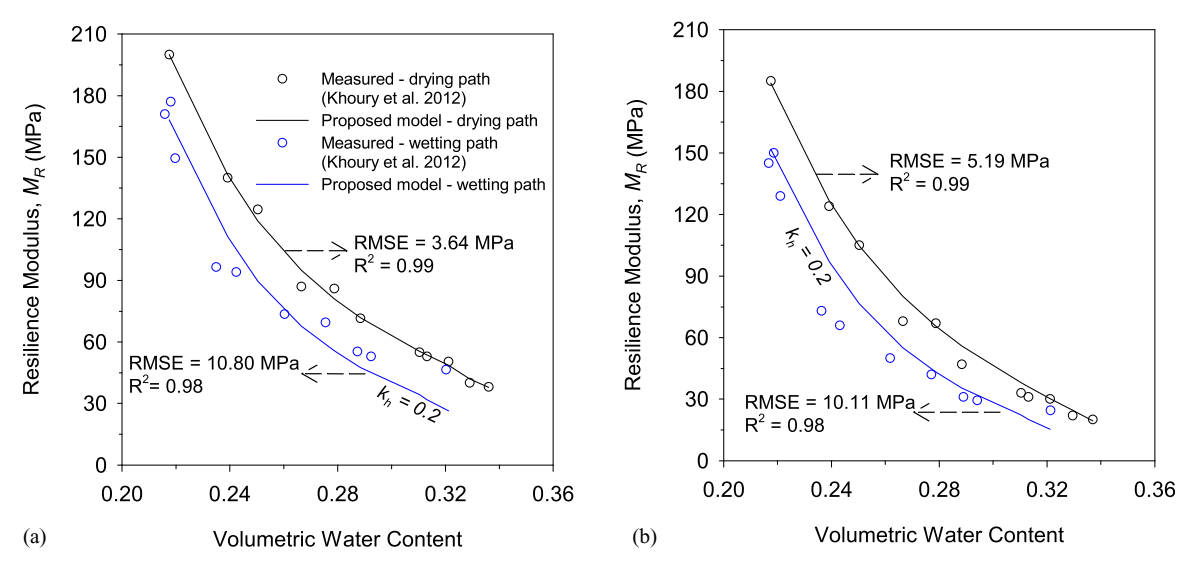


Fig. 11. Measured and predicted resilient modulus of Renfrow clay (Soil 14) along main wetting and drying curves at two different stress states: (a) θ_b = 154.6 kPa, $\tau_{\rm oct}$ = 13.0 kPa; and (b) θ_b = 83.0 kPa, $\tau_{\rm oct}$ = 19.3 kPa.

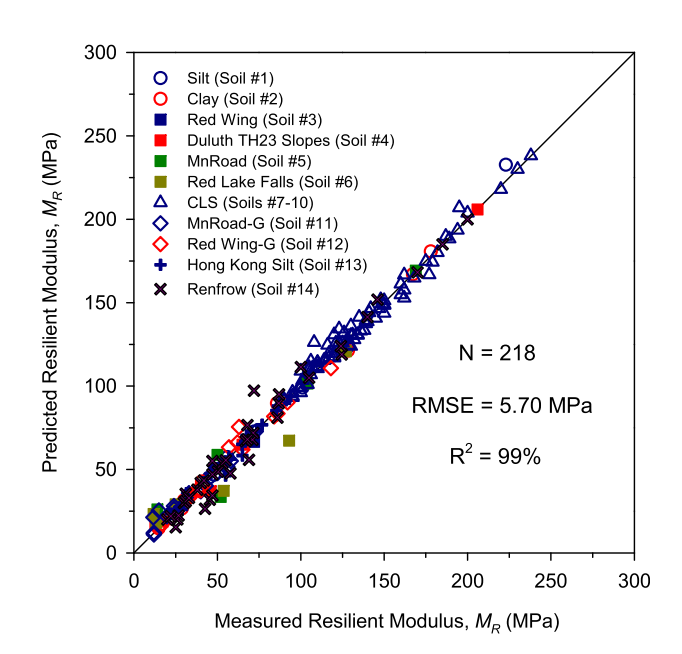


Fig. 12. Predicted using the proposed model versus measured resilient modulus for 14 soils.

OMC. The specimen was then dried to a moisture content of OMC–4% to achieve the initial drying curve. In the next step, the specimen was wetted to OMC+4% to achieve the main wetting curve. Finally, the specimen was dried back from OMC+4% to OMC–4% to obtain the main drying curve. Fig. 10 depicts the drying and wetting SWRCs of the soil based on the measured data reported by Zaman and Khoury (2007). Khoury et al. (2012) evaluated the effect of hysteresis moisture variations on the M_R values at two different stress levels: (1) a bulk stress (θ_b) of approximately 154.6 and 83.0 kPa and (2) corresponding octahedral shear stress ($\tau_{\rm oct}$) of 13.0 and 19.3 kPa. The suction level was controlled during the test using the axis-translation technique.

Fig. 11 shows a comparison between the measured and predicted M_R values of Renfrow clay (Soil 14) along main wetting and drying curves at two different stress states. In the proposed solution, M_R values obtained along the drying path are used as

reference points to predict the M_R values along the wetting path. As shown, M_R has higher values along the drying path. For each set, Fig. 11 includes R^2 and RMSE of the proposed model considering the effect of hysteresis. Results show that the proposed model can satisfactorily capture the effect of hydraulic hysteresis on M_R .

Overall Performance of Proposed Model

Fig. 12 provides a comparison between the experimentally measured M_R values reported in the literature versus those predicted using the proposed model in this study. A total of 218 measured data points are used in this study to evaluate the model performance considering the effects of water content, stress level, temperature, and hydraulic hysteresis on M_R . Fig. 12 shows an excellent agreement between the measured and predicted values with R^2 of 99% and RMSE of only 5.70 MPa. The results confirm that the proposed model offers a robust tool to account for the effects of various factors on M_R while addressing several limitations in the existing models. It is noted that confinement is implicitly considered in the proposed model through the resilient modulus at dry (M_{Md}) and saturated $(M_{R.SAT})$ states, which serve as upper and lower bounds respectively. These two values, M_{Md} and $M_{R,SAT}$, are functions of confining pressure and deviatoric stress for each soil. For instance, consider the parameters for Soil 14 in Table 2. Khoury et al. (2012) tested Soil 14 under different confining and deviatoric stresses. It can be seen that except for M_{Md} and $M_{R,SAT}$, all other fitting parameters are the same for this soil.

The proposed model is able to predict the M_R value for any type of subgrade soil knowing its water content. The model explicitly considers the effects of two water retention mechanisms of capillary and adsorption on soil stiffness, which enables it to predict the M_R value of subgrade soils over the entire range of water content much more accurate than alternative models including the MEPDG model. Furthermore, the model incorporates the effects of changes in deviatoric stress, temperature, and hysteresis. These factors are all important in assessing the pavement performance, because the subgrade soil beneath falls in the active zone where the water content and temperature are continuously changing under soil-climatic interactions. The presented model is developed upon the current state of the art in unsaturated soil mechanics, providing a theoretically sound yet practical basis for predicting M_R . The model can readily be adopted in guidelines such as AASHTO for analyzing the performance of existing

pavements, designing new pavements, and also performing forensic studies of failed pavements under various water content, temperature, and climatic conditions.

Conclusions

A general model is proposed in this study to capture the variation of the resilient modulus, M_R , with respect to the soil water content, stress level, temperature, and hydraulic hysteresis for compacted subgrade soils. It was shown that in low water content, development of high suctions significantly accelerates the hardening rate of M_R . The proposed model considers two different water retention mechanisms of capillarity and adsorption for the calculation of M_R . This feature enables the model to accurately capture the variation of M_R for various subgrade soils over the entire range of suction or degree of saturation. It was noted that M_R has a direct relationship with deviatoric stress. Having the M_R -water content curve at a reference deviatoric stress, the proposed model can predict the corresponding curve for other deviatoric stresses. It was shown that M_R decreased as the soil temperature increased. The proposed model can properly capture this behavior by considering the effect of temperature on water retention mechanisms. By linking to a temperature-dependent SWRC, the proposed model is extended to consider the effect of temperature on M_R , a feature that none of the existing models offers. The proposed model can also account for the effect of hydraulic hysteresis on M_R by linking the effect of wetting and drying cycles on the SWRC to resilient modulus.

Measured data for 14 different subgrade soils reported in the literature are used to examine the performance of the proposed model. The comparison demonstrates an excellent accuracy for the proposed predictive model ($R^2 = 99\%$), with errors significantly lower than those from four alternative models. The model uses the volumetric water content as a direct input, which, unlike suction, is commonly measured in field conditions. This can facilitate the widespread application of the model in practice. The proposed model is straightforward and can be used in practice to design pavements over unsaturated subgrade soils.

Data Availability Statement

All data, models, and code generated or used during the study appear in the published article.

Acknowledgments

This material is based upon work supported in part by the National Science Foundation under Grant No. CMMI-1951636. Any opinions, findings, and conclusions or recommendations expressed in this material are those of the authors and do not necessarily reflect the views of the National Science Foundation.

Notation

The following symbols are used in this paper:

 a_{FX} , n_{FX} , = Fredlund and Xing (1994) SWRC model's fitting

 m_{FX} parameters;

 k_h = fitting parameter considering the effect of hydraulic hysteresis [Eq. (23)];

 k_m = fitting parameter considering the changes in moisture content [Eq. (2)];

 k_1 , k_2 , k_3 = MEPDG model fitting parameters [Eq. (1)];

 l_1 , l_2 = Yang et al. (2005) model fitting parameters [Eq. (3)];

m = SWRC fitting parameters reflecting adsorption strength;

 m_M = fitting parameter considering the effect of capillary water content [Eq. (11)];

 M_{Mc} = maximum resilient modulus due to capillary mechanism;

 M_{Md} = maximum resilient modulus at dry state;

 M_R = resilient modulus;

 $(M_R)_D$ = resilient modulus along the main drying path;

 $(M_R)_W$ = resilient modulus along the main wetting path;

 $M_{R,OPT}$ = resilience modulus at optimum moisture content;

 $M_{R,SAT}$ = resilient modulus at saturated condition;

 $M_w = \text{molar volume of water};$

 m_1 , m_2 , m_3 = Liang et al. (2008) model fitting parameters [Eq. (4)];

n = SWRC fitting parameters related to soil particle size and distribution;

 $n_1, n_2, n_3, n_4 = \text{Cary and Zapata (2011) model fitting parameters}$ [Eq. (5)];

 P_a = atmospheric pressure;

R = universal gas constant;

 R^2 = coefficient of determination;

RH = relative humidity;

RMSE = root mean square error;

S =degree of saturation;

 S_{OPT} = degree of saturation at optimum moisture content;

T = temperature;

 Δh_T = enthalpy of immersion per unit area;

 Δh_{T_r} = enthalpy of immersion per unit area at the reference temperature;

 $\Delta u_{w\text{-sat}}$ = buildup of pore-water pressure under saturated condition;

 $\alpha = \text{SWRC}$ fitting parameters related to soil air entry

 α' = soil-water contact angle;

 β , β_{T_r} = regression parameters of Eq. (18);

 ε_r = recoverable strain;

 κ = fitting parameter considering the effect of changes in deviatoric stress [Eq. (15)];

 θ = volumetric water content;

 $\theta_{a,\text{max}}$ = maximum adsorption water content;

 θ_b = bulk stress;

 $\theta_{\text{net}} = \text{net bulk stress};$

 θ_s = saturated volumetric water content;

 ξ = Han and Vanapalli (2015) model fitting parameter [Eq. (6)];

 σ_d = deviatoric stress;

 $\tau_{\rm oct}$ = octahedral shear stress;

 χ = Bishop's effective stress parameter;

 ψ = suction;

 ψ_c = mean cavitation pressure;

 ψ_D = suction along main wetting path;

 $\psi_{\text{max}} = \text{maximum suction};$

 ψ_{OPT} = suction at optimum moisture content;

 $\psi_{T_{*}}$ = reference temperature; and

 ψ_W = suction along main drying path.

References

AASHTO. 1993. Guide for design of pavement structures. Washington, DC: AASHTO.

- AASHTO. 2003. Determining the resilient modulus of soils and aggregate materials. T307 99, standard specifications for transportation materials and methods of sampling and testing. Washington, DC: AASHTO.
- AASHTO. 2012. Determining the resilient modulus of soils and aggregate. AASHTO T-307. Washington, DC: AASHTO.
- Alonso, E. E., E. Romero, C. Hoffmann, and E. García-Escudero. 2005. "Expansive bentonite—sand mixtures in cyclic controlled-suction drying and wetting." *Eng. Geol.* 81 (3): 213–226. https://doi.org/10.1016/j .enggeo.2005.06.009.
- Banerjee, A., A. J. Puppala, S. S. C. Congress, S. Chakraborty, W. J. Likos, and L. R. Hoyos. 2020a. "Variation of resilient modulus of subgrade soils over a wide range of suction states." *J. Geotech. Geoenviron. Eng.* 146 (9): 4020096. https://doi.org/10.1061/(ASCE)GT.1943-5606.0002332.
- Banerjee, A., A. J. Puppala, L. R. Hoyos, W. J. Likos, and U. D. Patil. 2020b. "Resilient modulus of expansive soils at high suction using vapor pressure control." *Geotech. Test. J.* 43 (3): 720–736. https://doi.org/10.1520/GTJ20180255.
- Blackmore, L., C. R. Clayton, W. Powrie, J. A. Priest, and L. Otter. 2020. "Saturation and its effect on the resilient modulus of a pavement formation material." *Géotechnique* 70 (4): 292–302. https://doi.org/10.1680/jgeot.18.P.053.
- Caicedo, B., O. Coronado, J. M. Fleureau, and A. G. Correia. 2009. "Resilient behaviour of non standard unbound granular materials." *Road Mater. Pavement Des.* 10 (2): 287–312. https://doi.org/10.1080/14680629.2009.9690196.
- Cao, T. C., S. K. Thota, F. Vahedifard, and A. Amirlatifi. 2021. "A temperature-dependent model for thermal conductivity function of unsaturated soils." In *Proc.*, 2021 Int. Foundations Congress and Equipment Exposition, Geotechnical Special Publication 325, edited by C. El Mohtar, S. Kulesza, T. Baser, and M. D. Venezia, 89–98. Reston, VA: ASCE.
- Cary, C. E., and C. E. Zapata. 2011. "Resilient modulus for unsaturated unbound materials." *Road Mater. Pavement Des.* 12 (3): 615–638. https://doi.org/10.1080/14680629.2011.9695263.
- Chu, X. 2020. "A review on the resilient response of unsaturated subgrade soils." Adv. Civ. Eng. 2020: 7367484. https://doi.org/10.1155/2020 /7367484
- Dong, Y., and N. Lu. 2016. "Correlation between small-strain shear modulus and suction stress in capillary regime under zero total stress conditions." J. Geotech. Geoenviron. Eng. 142 (11): 04016056. https://doi .org/10.1061/(ASCE)GT.1943-5606.0001531.
- Dorsey, N. E. 1940. *Properties of ordinary water substance*. New York: Reinhold.
- Esfandiari, Z., M. Ajdari, and F. Vahedifard. 2021. "Time-dependent deformation characteristics of unsaturated sand–bentonite mixture under drying–wetting cycles." *J. Geotech. Geoenviron. Eng.* 147 (3), 04020172. https://doi.org/10.1061/(asce)gt.1943-5606.0002455.
- Everett, D. H. 1972. "Definitions, terminology and symbols in colloid and surface chemistry." *Pure Appl. Chem.* 31 (4): 577–638. https://doi.org /10.1351/pac197231040577.
- Francois, B., and L. Laloui. 2008. "ACMEG-TS: A constitutive model for unsaturated soils under non-isothermal conditions." Int. J. Numer. Anal. Methods Geomech. 32 (16): 1955–1988. https://doi.org/10.1002/nag.712.
- Fredlund, D. G., A. T. Bergan, and P. K. Wong. 1977. "Relation between resilient modulus and stress conditions for cohesive subgrade soils." *Transp. Res. Rec.* 642: 73–81.
- Fredlund, D. G., and A. Xing. 1994. "Equations for the soil-water characteristic curve." *Can. Geotech. J.* 31 (4): 521–532. https://doi.org/10.1139/t94-061.
- Freitas, J. B., L. R. Rezende, and G. Gitirana. 2020. "Prediction of the resilient modulus of two tropical subgrade soils considering unsaturated conditions." *Eng. Geol.* 270: 105580. https://doi.org/10.1016/j.enggeo.2020.105580.
- George, K. P. 2004. Prediction of resilient modulus from soil index properties. Rep. No. FHWA/MS-DOT-RD-04-172. Washington, DC: FHWA, Dept. of Transportation.
- Goodman, C. C., and F. Vahedifard. 2019. "Micro-scale characterisation of clay at elevated temperatures." Géotech. Lett. 9 (3): 225–230. https://doi .org/10.1680/jgele.19.00026.

- Grant, S. A., and A. Salehzadeh. 1996. "Calculation of temperature effects on wetting coefficients of porous solids and their capillary pressure functions." Water Resour. Res. 32 (2): 261–270. https://doi.org/10 .1029/95WR02915.
- Gupta, S. C., A. Ranaivoson, T. B. Edil, C. H. Benson, and A. Sawangsuriya. 2007. Pavement design using unsaturated soil technology. St. Paul, MN: Minnesota Dept. of Transportation.
- Haar, L., J. S. Gallagher, and G. S. Kell. 1984. NBS/NRC steam table. New York: Hemisphere Publishing Corporation.
- Han, Z., and S. K. Vanapalli. 2015. "Model for predicting resilient modulus of unsaturated subgrade soil using soil-water characteristic curve." *Can. Geotech. J.* 52 (10): 1605–1619. https://doi.org/10.1139/cgj-2014-0339.
- Han, Z., and S. K. Vanapalli. 2016. "State-of-the-art: Prediction of resilient modulus of unsaturated subgrade soils." *Int. J. Geomech.* 16 (4): 04015104. https://doi.org/10.1061/(ASCE)GM.1943-5622.0000631.
- Jeppu, G. P., and T. P. Clement. 2012. "A modified Langmuir-Freundlich isotherm model for simulating pH-dependent adsorption effects." *J. Contam. Hydrol.* 129–130: 46–53. https://doi.org/10.1016/j.jconhyd. .2011.12.001.
- Jin, M. S., W. D. Kovacs, and K. W. Lee. 1994. "Seasonal variation of resilient modulus of subgrade soils." *J. Transp. Eng.* 120 (4): 603–616. https://doi.org/10.1061/(ASCE)0733-947X(1994)120:4(603).
- Khosravi, A., and J. S. McCartney. 2012. "Impact of hydraulic hysteresis on the small-strain shear modulus of low plasticity soils." *J. Geotech. Geoenviron. Eng.* 138 (11): 1326–1333. https://doi.org/10.1061/(ASCE)GT.1943-5606.0000713.
- Khoury, N., R. Brooks, C. Khoury, and D. Yada. 2012. "Modeling resilient modulus hysteretic behavior with moisture variation." *Int. J. Geomech*. 12 (5): 519–527. https://doi.org/10.1061/(ASCE)GM.1943-5622.0000140.
- Khoury, N. N., and M. M. Zaman. 2004. "Correlation between resilient modulus, moisture variation, and soil suction for subgrade soils." *Transp. Res. Rec.* 1874 (1): 99–107. https://doi.org/10.3141/1874-11.
- Liang, R. Y., S. Rabab'ah, and M. Khasawneh. 2008. "Predicting moisture-dependent resilient modulus of cohesive soils using soil suction concept." *J. Transp. Eng.* 134 (1): 34–40. https://doi.org/10.1061/(ASCE) 0733-947X(2008)134:1(34).
- Lu, N. 2016. "Generalized soil water retention equation for adsorption and capillarity." J. Geotech. Geoenviron. Eng. 142 (10): 04016051. https:// doi.org/10.1061/(ASCE)GT.1943-5606.0001524.
- Lu, N. 2018. "Generalized elastic modulus equation for unsaturated soil." In *Proc., 2nd Pan-American Conf. on Unsaturated Soils*, Geotechnical Special Publication 300, edited by L. R. Hoyos, J. S. McCartney, S. L. Houston, and W. J. Likos, 32–48. Reston, VA: ASCE.
- Lu, N., and M. Kaya. 2014. "Power law for elastic moduli of unsaturated soil." J. Geotech. Geoenviron. Eng. 140 (1): 46–56. https://doi.org/10 .1061/(ASCE)GT.1943-5606.0000990.
- Lu, N., and W. J. Likos. 2004. *Unsaturated soil mechanics*. New York: Wiley.
- Mathews, J., and R. L. Walker. 1970. Vol. 501 of Mathematical methods of physics. New York: WA Benjamin.
- McCartney, J. S., N. H. Jafari, T. Hueckel, M. Sanchez, and F. Vahedifard. 2019. "Thermal energy issues in geotechnical engineering." In Geotechnical fundamentals for addressing new world challenges, edited by N. Lu, and J. K. Mitchell, 275–317. Dordrecht, Netherlands: Springer.
- McCartney, J. S., and A. Khosravi. 2013. "Field-monitoring system for suction and temperature profiles under pavements." *J. Perform. Construct. Facil.* 27 (6): 818–825. https://doi.org/10.1061/(ASCE)CF .1943-5509.0000362.
- Miao, Y. H., Y. C. Huang, Q. Q. Zhang, and L. B. Wang. 2016. "Effect of temperature on resilient modulus and shear strength of unbound granular materials containing fine RAP." *Constr. Build Mater.* 124: 1132– 1141. https://doi.org/10.1016/j.conbuildmat.2016.08.137.
- Monghassem, M., M. Ajdari, S. M. Binesh, and F. Vahedifard. 2021. "Effects of suction and drying-wetting cycles on shearing response of adobe." *J. Mater. Civ. Eng.* 33 (7): 04021173. https://doi.org/10.1061 /(asce)mt.1943-5533.0003816.
- Nazzal, M. D., and L. N. Mohammad. 2010. "Estimation of resilient modulus of subgrade soils for design of pavement structures." *J. Mater. Civ. Eng.* 229 (7): 726–734. https://doi.org/10.1061/(ASCE)MT.1943-5533.0000073.

- NCHRP (National Cooperative Highway Research Program). 2003. Harmonized test method for laboratory determination of resilient modulus for flexible pavement design. Final Rep. NCHRP 1-28A. Washington, DC: TRB, National Research Council.
- NCHRP (National Cooperative Highway Research Program). 2004. *Guide for mechanistic–empirical design of new and rehabilitated pavement structures*. Project No. 1-37A, Prepared by ARA, Inc., ERES Consultants Division. Washington, DC: NCHRP Transportation Research Board.
- Ng, C. W. W., and C. Zhou. 2014. "Cyclic behavior of an unsaturated silt at various suctions and temperatures." *Géotechnique* 64 (9): 709–720. https://doi.org/10.1680/geot.14.P.015.
- Ng, C. W. W., C. Zhou, Q. Yuan, and J. Xu. 2013. "Resilient modulus of unsaturated subgrade soil: Experimental and theoretical investigations." *Can. Geotech. J.* 50 (2): 223–232. https://doi.org/10.1139/cgj-2012 -0052.
- Nitao, J. J., and J. Bear. 1996. "Potentials and their role in transport in porous media." Water Resour. Res. 32 (2): 225–250. https://doi.org/10.1029/95WR02715.
- Pasha, A. Y., A. Khoshghalb, and N. Khalili. 2017. "Hysteretic model for the evolution of water retention curve with void ratio." *J. Eng. Mech.* 143 (7): 04017030. https://doi.org/10.1061/(ASCE)EM.1943-7889 .0001238.
- Ponec, V., Z. Knor, and S. Cerny. 1974. *Adsorption on solids*. London: Butterworth and Co.
- Puppala, A. J. 2008. Estimating stiffness of subgrade and unbound materials for pavement design. NCHRP Synthesis 382. Washington, DC:
 National Cooperative Highway Research Program, Transportation Research Board.
- Puppala, A. J., T. Manosuthkij, S. Nazarian, and L. R. Hoyos. 2011. "Threshold moisture content and matric suction potentials in expansive clays prior to initiation of cracking in pavements." *Can. Geotech. J.* 48 (4): 519–531. https://doi.org/10.1139/t10-087.
- Revil, A., and N. Lu. 2013. "Unified water isotherms for clayey porous materials." Water Resour. Res. 49 (9): 5685–5699. https://doi.org/10.1002/wrcr.20426.
- Romero, E., A. Gens, and A. Lloret. 2001. "Temperature effects on the hydraulic behavior of an unsaturated clay." *Geotech. Geol. Eng.* 19 (3/4): 311–332. https://doi.org/10.1023/A:1013133809333.
- Sahin, H., F. Gu, Y. Tong, and R. L. Lytton. 2013. "Unsaturated soil mechanics in the design and performance of pavements." In *Proc., 1st Pan-Am. Conf. on Unsaturated Soils*, Rotterdam, Netherlands: A.A. Balkema.
- Salager, S., M. S. Ei Youssoufi, and C. Saix. 2007. "Influence of temperature on the water retention curve of soils. Modelling and experiments." In *Experimental unsaturated soil mechanics*, edited by T. Schanz, 251–258. Berlin: Springer.
- Salimi, K., A. Cerato, F. Vahedifard, and G. Miller. 2021a. "Tensile strength of compacted clays during desiccation under elevated temperatures." *Geotech. Test. J.* 44 (4): 1119–1134. https://doi.org/10.1520/gtj20200114.
- Salimi, K., A. Cerato, F. Vahedifard, and G. A. Miller. 2021b. "A temperature-dependent model for tensile strength characteristic curve of unsaturated soils." *Geomech. Energy Environ*. 28: 100244. https:// doi.org/10.1016/J.GETE.2021.100244.
- Sawangsuriya, A., T. B. Edil, and C. H. Benson. 2009. "Effect of suction on resilient modulus of compacted fine-grained subgrade soils." *Transp. Res. Rec.* 2101 (1): 82–87. https://doi.org/10.3141/2101-10.
- Schneider, M., and K.-U. Goss. 2011. "Temperature dependence of the water retention curve for dry soils." *Water Resour. Res.* 47: W03506. https://doi.org/10.1029/2010WR009687.

- Seed, H. B., C. K. Chan, and C. E. Lee. 1962. "Resilience characteristics of subgrade soils and their relation to fatigue failures in asphalt pavements." In *Proc., Int. Conf. on the Structural Design of Asphalt Pavements*, 611–636. Reston, VA: ASCE.
- Tang, C.-S., D.- Y. Wang, B. Shi, and J. Li. 2016. "Effect of wetting-drying cycles on profile mechanical behavior of soils with different initial conditions." *CATENA* 139: 105–116. https://doi.org/10.1016/j.catena .2015.12.015.
- Tarantino, A. 2009. "A water retention model for deformable soils." Geotechnique 59 (9): 751–762. https://doi.org/10.1680/geot.7.00118.
- Thota, S. K., T. C. Cao, F. Vahedifard, and E. Ghazanfari. 2020. "An effective stress model for unsaturated soils at elevated temperatures." In Proc., Geo-Congress 2020: Geo-Systems, Sustainability, Geoenvironmental Engineering, and Unsaturated Soil Mechanics, Geotechnical Special Publication No. 319, edited by J. P. Hambleton, R. Makhnenko, and A. S. Budge, 358–366. Reston, VA: ASCE.
- Tuller, M., D. Or, and L. M. Dudley. 1999. "Adsorption and capillary condensation in porous media: Liquid retention and interfacial configurations in angular pores." *Water Resour. Res.* 35 (7): 1949–1964. https://doi.org/10.1029/1999WR900098.
- Vahedifard, F., T. D. Cao, E. Ghazanfari, and S. K. Thota. 2019. "Closed-form models for nonisothermal effective stress of unsaturated soils." *J. Geotech. Geoenviron. Eng.* 145 (9): 04019053. https://doi.org/10.1061/(ASCE)GT.1943-5606.0002094.
- Vahedifard, F., C. T. Duc, T. S. Kumar, and E. Ghazanfari. 2018. "Nonisothermal models for soil–water retention curve." *J. Geotech. Geoenviron. Eng.* 144 (9): 04018061. https://doi.org/10.1061/(ASCE) GT.1943-5606.0001939.
- Vahedifard, F., S. K. Thota, T. C. Cao, R. A. Samarakoon, and J. S. McCartney. 2020. "A temperature-dependent model for small-strain shear modulus of unsaturated soils." *J. Geotech. Geoenviron. Eng.* 146 (12): 04020136. https://doi.org/10.1061/(asce)gt.1943-5606.0002406.
- van Genuchten, M. T. 1980. "A closed-form equation for predicting the hydraulic conductivity of unsaturated soils." *Soil Sci. Soc. Am. J.* 44 (5): 892–898. https://doi.org/10.2136/sssaj1980.03615995004400050002x.
- Watson, K. M. 1943. "Thermodynamics of the liquid state." *Ind. Eng. Chem.* 35 (4): 398–406. https://doi.org/10.1021/ie50400a004.
- Yang, S. R., W. H. Huang, and Y. T. Tai. 2005. "Variation of resilient modulus with soil suction for compacted subgrade soils." *Transp. Res. Rec.* 1913 (1): 99–106. https://doi.org/10.1177/0361198105191300110.
- Yao, Y., J. Zheng, J. Zhang, J. Peng, and J. Li. 2018. "Model for predicting resilient modulus of unsaturated subgrade soils in south China." KSCE J. Civ. Eng. 22 (6): 2089–2098. https://doi.org/10.1007/s12205-018 -1703-1.
- Zaman, M., and N. Khoury. 2007. Effect of soil suction and moisture on resilient modulus of subgrade soils in Oklahoma. Rep. No. ORA 125-6662. Norman, OK: Oklahoma Dept. of Transportation.
- Zhang, C., and N. Lu. 2020. "Unified effective stress equation for soil."
 J. Eng. Mech. 146 (2): 04019135. https://doi.org/10.1061/(ASCE)EM
 .1943-7889.0001718.
- Zhang, J., J. Peng, W. Liu, and W. Lu. 2021. "Predicting resilient modulus of fine-grained subgrade soils considering relative compaction and matric suction." *Road Mater. Pavement Des.* 22 (3): 703–715. https://doi.org/10.1080/14680629.2019.1651756.
- Zhou, A.-N., D. Sheng, and J. Li. 2014. "Modelling water retention and volume change behaviours of unsaturated soils in non-isothermal conditions." *Comput. Geotech.* 55: 1–13. https://doi.org/10.1016/j.compgeo.2013.07.011.
- Zhou, C., and C. W. Ng. 2016. "Simulating the cyclic behaviour of unsaturated soil at various temperatures using a bounding surface model." *Géotechnique* 66 (4): 344–350. https://doi.org/10.1680/jgeot.15.P.001.